



ORAU TEAM Dose Reconstruction Project for NIOSH

Oak Ridge Associated Universities | Dade Moeller | MJW Technical Services

Page 1 of 68

DOE Review Release 02/20/2014

Document Title: Response of Dosimeters to Aged Fission Products in a Tank Farm Environment at the Savannah River Site	Document Number: ORAUT-RPRT-0062 Revision: 00 Effective Date: 02/11/2014 Type of Document: Report Supersedes: None
Subject Expert(s): James M. Mahathy, Roger Halsey, Robert L. Morris	
Approval:	Signature on File James M. Mahathy, Document Owner
Concurrence:	Signature on File Daniel H. Stempfley, Objective 4 Representative
Concurrence:	Vickie S. Short Signature on File for Kate Kimpan, Project Director
Approval:	Signature on File James W. Neton, Associate Director for Science

New Total Rewrite Revision Page Change

FOR DOCUMENTS MARKED AS A TOTAL REWRITE, REVISION, OR PAGE CHANGE, REPLACE THE PRIOR REVISION AND DISCARD / DESTROY ALL COPIES OF THE PRIOR REVISION.

PUBLICATION RECORD

EFFECTIVE DATE	REVISION NUMBER	DESCRIPTION
02/11/2014	00	New report initiated to document the response of the Savannah River Site multielement film dosimeter to external penetrating photon radiation in the tank farm environment. Incorporates formal internal and NIOSH review comments. Training required: As determined by the Objective Manager. Initiated by James M. Mahathy.

TABLE OF CONTENTS

<u>SECTION</u>	<u>TITLE</u>	<u>PAGE</u>
Acronyms and Abbreviations		5
1.0 Introduction		6
2.0 Fission Product Source		6
2.1 Photons		6
2.2 Bremsstrahlung Photons		9
2.3 Combined Gamma and X-ray Photon Spectrum.....		9
2.4 Mathematical Model of the Work Environment.....		9
2.5 Results		12
2.6 Glovebag Data		15
2.7 Mathematical Model of the Dosimeter.....		17
2.8 Dosimeter Response		18
3.0 Summary		20
4.0 Organ Dose Conversion Factors		21
5.0 Conclusions		21
References		22
ATTACHMENT A, ENERGY SPECTRA CALCULATED FROM TANK MODELS FOR FILM BADGE MODELS.....		24
ATTACHMENT B, DOSE MODELS		28
ATTACHMENT C, FILM BADGE MODEL.....		63

LIST OF TABLES

<u>TABLE</u>	<u>TITLE</u>	<u>PAGE</u>
2-1	ORIGEN-S irradiation parameters for the five SRS cases	6
2-2	Fission product mixture used to define the radiation source term	7
2-3	Intensity of gamma and X-ray components of the photon spectrum	8
2-4	Tank contents—elements and relative abundances	10
2-5	Dose ratios for the 30- to 250-keV energy range.....	14
2-6	Dose ratios for the greater than 250-keV energy range	14
2-7	The fractions of total dose by energy range for each scenario	15
2-8	Survey readings taken above ports on SRS tanks	16
2-9	Silver-shielded film ratios	20
A-1	Standing worker, no port, 140 and 90 cm.....	24
A-2	Kneeling worker, no port, 90 and 40 cm	25
A-3	Standing worker, near port, 140 and 90 cm.....	26
A-4	Kneeling worker, near port, 90 and 40 cm.....	27

LIST OF FIGURES

<u>FIGURE</u>	<u>TITLE</u>	<u>PAGE</u>
2-1	Semi-log plot of the combined photon spectrum.....	8
2-2	Cross-sectional diagram of a Type III tank	9
2-3	SRS workers measuring the level of waste in a tank	11
2-4	Model of standing worker	11
2-5	Model of kneeling worker	11
2-6	Standing worker, no port	12
2-7	Kneeling worker, no port	12
2-8	Standing worker, near a port	13
2-9	Kneeling worker, near a port	13
2-10	Diagram of glovebag and reading locations	16
2-11	Ratios from Survey Forms and MCNP calculations	17
2-12	Exploded view of SRS film badge model.....	18
2-13	Comparison of the actual curve of two-element film dosimeter OW response to an MCNP simulation	19

ACRONYMS AND ABBREVIATIONS

AP	anterior-posterior
cm	centimeter
d	day
DOE	U.S. Department of Energy
g	gram
ICRP	International Commission on Radiological Protection
keV	kiloelectron-volt, 1,000 electron-volts
MCNP	Monte Carlo N-Particle (computer program)
MeV	megaelectron-volt, 1 million electron-volts
mm	millimeter
MTU	metric tons of uranium
MW	megawatt
MWd	megawatt-day
NIOSH	National Institute for Occupational Safety and Health
NTA	nuclear track emulsion, Type A
ORAU	Oak Ridge Associated Universities
OW	open window
ROT	rotational
SRDB Ref ID	Site Research Database Reference Identification (number)
SRS	Savannah River Site

1.0 INTRODUCTION

At the Savannah River Site (SRS), liquid wastes containing fission products were stored in large underground tanks. When a worker was in the Tank Farm area and the dosimeter was routinely worn at the worker's collar, it is reasonable to expect based on distance from the below source that it will record a lower dose in comparison with a dosimeter worn at the worker's beltline. In addition, when near an open sampling port, the badge can overestimate the dose at the abdomen due to the streaming effect of a beam created by the opening. The differences in response as a function of position on the worker's torso were evaluated using the MCNP5 code, version 1.60 and MCNPX code, version 2.6.0. MCNP is a Fortran90 Monte Carlo radiation transport computer code developed and maintained by Los Alamos National Laboratory.

2.0 FISSION PRODUCT SOURCE

The fission product source represents external penetrating photons from gamma rays and bremsstrahlung X-rays associated with high-energy beta emitters.

The fission product mixture that was used to develop the source term was extracted from the ORIGEN-S program for the SRS reactors. Two sets of irradiation parameters were selected for the Mark 16 and Mark VI-B cases. The selected irradiation parameters for the five SRS cases are given in Table 2-1. For each reactor, the inventory was normalized to the ^{137}Cs activity and then averaged across all reactors to provide an estimate of the expected source that would have been encountered. All radionuclides from ORIGEN-S that have activity for the SRS reactor cases were used. Table 2-2 shows SRS reactor radionuclides and their relative activities normalized to the activity of ^{137}Cs . Table 2-2 is sorted by highest average relative activity to ^{137}Cs . Note that about 90% of the total activity comes from the first 10 radionuclides through ^{137}Cs . The beta emitter ^{90}Sr and its equilibrated progeny ^{90}Y are also included in the fission product source term due to their relatively high abundance and ability to produce bremsstrahlung X-rays.

Table 2-1. ORIGEN-S irradiation parameters for the five SRS cases.

Case	Parameters	Basis
Mark V-B	Specific power = 25.5 MW/MTU Irradiation time = 43.14 d Burnup = 1,100 MWd/MTU	Production of weapons-grade plutonium (nominal 6% ^{240}Pu content) at nominal power.
Mark 16 1	Specific power = 896.08 MW/MTU Irradiation time = 240 d Burnup = 215,059 MWd/MTU	Typical Mark 16/31 core irradiated for four subcycles of 60 days each, representing the high-burnup case.
Mark 16 2	Specific power = 896.08 MW/MTU Irradiation time = 160 d Burnup = 143,373 MWd/MTU	Typical Mark 16/31 core irradiated for four subcycles of 40 days each, representing the low-burnup case.
Mark VI-B 1	Specific power = 1392.9 MW/MTU Irradiation time = 182 d Burnup = 253,508 MWd/MTU	Maximum assembly power for a typical cycle duration.
Mark VI-B 2	Specific power = 1160.32 MW/MTU Irradiation time = 182 d Burnup = 211,178 MWd/MTU	Nominal assembly power for a typical cycle duration.

2.1 PHOTONS

The gamma and X-ray photon contributions for all radionuclides in Table 2-2 were used to create a 30-segment histogram spectrum, which is shown in Table 2-3 and Figure 2-1. Radiation data tables were taken from the freeware program RADDECAY.EXE (Radiation Decay, Version 3.6).

RADDECAY uses data from DOE/TIC-11026, *Radioactive Decay Data Tables, A Handbook of Decay Data for Application to Radiation Dosimetry and Radiological Assessments* (Kocher 1981).

Table 2-2. Fission product mixture used to define the radiation source term. Activity units are relative to ^{137}Cs , which is normalized to equal 1. Table includes noble gases and volatile species regardless of whether they would actually be present in the tank farm wastes.

Radionuclide	Average activity						
Pr-144	1.18E+01	C-14	9.91E-06	Ag-108m	2.20E-11	Te-123	2.55E-19
Ce-144	1.18E+01	Ni-59	7.35E-06	Dy-159	1.91E-11	Xe-133	2.00E-19
Nb-95	3.74E+00	Ag-110	6.47E-06	Xe-127	1.39E-11	Tc-95m	1.57E-19
Pm-147	2.58E+00	Cd-113m	4.58E-06	Te-121m	1.07E-11	Ag-105	1.14E-19
Zr-95	1.74E+00	Gd-153	3.99E-06	Te-121	1.06E-11	Cs-131	8.55E-20
Ru-106	1.18E+00	Cr-51	3.98E-06	Sn-117m	7.36E-12	S-35	2.12E-20
Rh-106	1.18E+00	Sn-126	2.98E-06	La-137	6.44E-12	Tc-95	6.20E-21
Y-91	1.11E+00	Sb-126m	2.98E-06	Tc-98	6.42E-12	Sc-46	2.18E-21
Cs-137	1.00E+00	Rh-102	2.32E-06	Tb-157	5.77E-12	Cs-132	1.58E-21
Y-90	9.67E-01	Cs-135	1.89E-06	Se-75	4.29E-12	Ga-68	4.82E-22
Sr-90	9.66E-01	Pr-143	1.10E-06	As-73	2.91E-12	Ge-68	4.82E-22
Ba-137m	9.44E-01	Nb-93m	1.04E-06	Ag-108	1.91E-12	Ba-131	1.26E-22
Sr-89	4.77E-01	Pm-146	9.47E-07	P-32	1.53E-12	V-50	4.74E-23
Cs-134	4.51E-01	Se-79	7.48E-07	I-131	1.51E-12	Eu-147	1.87E-23
Pr-144m	1.65E-01	Sb-126	4.18E-07	Si-32	1.51E-12	Ag-106m	8.34E-25
Kr-85	1.23E-01	La-140	3.75E-07	Sn-125	1.21E-12	Rh-99	3.26E-25
Ru-103	9.05E-02	Te-123m	3.58E-07	Be-7	8.53E-13	Tm-167	6.28E-27
Rh-103m	9.03E-02	Ba-140	3.26E-07	Pd-103	3.90E-13	Sb-120m	4.83E-27
Sb-125	4.88E-02	Pd-107	1.89E-07	Kr-81	1.97E-13	K-42	5.62E-28
Ce-141	4.38E-02	I-129	1.80E-07	Tm-168	1.09E-13	Ar-42	5.62E-28
Te-127m	3.18E-02	Tm-171	1.66E-07	Zr-88	1.08E-13	Cl-36	4.98E-28
Te-127	3.12E-02	Y-88	1.30E-07	Pm-144	9.20E-14	Sb-127	1.28E-28
Nb-95m	2.05E-02	Eu-156	1.10E-07	Eu-149	5.84E-14	Tb-156	1.47E-30
Eu-154	1.85E-02	Ag-109m	8.13E-08	I-125	5.32E-14	Gd-149	1.57E-31
Eu-155	1.49E-02	Cd-109	8.13E-08	V-49	3.15E-14	Lu-171	6.35E-32
Te-125m	1.18E-02	Ce-139	2.78E-08	Ho-163	2.94E-14	Tb-155	2.24E-32
Fe-55	8.38E-03	Rb-86	2.66E-08	Nb-91	1.50E-14	I-132	1.97E-32
Sm-151	4.72E-03	Tm-170	1.65E-08	Sm-146	1.42E-14	Te-132	1.91E-32
H-3	4.19E-03	Nd-147	4.75E-09	Nd-144	9.91E-15	Lu-172	6.71E-34
Zn-65	3.56E-03	In-115m	3.53E-09	Na-22	9.02E-15	Ar-39	1.27E-34
Sn-123	2.06E-03	Pm-145	2.98E-09	As-74	6.40E-15	Ar-37	5.20E-35
Te-129m	1.05E-03	Cs-136	2.20E-09	I-126	3.74E-15	Rh-101m	4.12E-36
Pm-148m	9.82E-04	Be-10	1.84E-09	Mo-93	3.71E-15	Ho-166	1.54E-36
Ni-63	9.17E-04	Rb-83	1.32E-09	Tc-97	2.33E-15	Dy-166	1.04E-36
Te-129	6.75E-04	Xe-131m	1.31E-09	Ag-111	1.80E-15	Mo-99	1.41E-38
Ag-110m	4.76E-04	Ba-133	1.27E-09	La-138	1.47E-15	Tc-99m	1.37E-38
Mn-54	4.66E-04	Rb-84	1.16E-09	P-33	1.15E-15	Ca-41	8.69E-39
Co-58	3.52E-04	Rh-102m	6.04E-10	In-113m	2.59E-16	Sc-47	5.37E-39
Sn-119m	1.51E-04	In-114m	2.77E-10	Sn-113	2.58E-16	K-40	2.34E-39
Tc-99	1.42E-04	In-114	2.65E-10	In-115	1.19E-16	Ca-47	1.41E-39
Sn-121m	6.95E-05	Rb-87	2.61E-10	Sm-148	1.16E-16	I-124	6.60E-40
Sn-121	5.39E-05	Ba-136m	2.47E-10	Er-169	3.76E-17	Zr-89	2.56E-40
Pm-148	5.20E-05	Nb-94	1.58E-10	Xe-129m	3.38E-17	Tc-96	2.27E-40
Sb-124	4.44E-05	Sr-85	1.42E-10	Nb-92	2.87E-17	Te-118	5.53E-41
Y-89m	4.43E-05	Tc-97m	1.13E-10	Ge-71	2.31E-17	Sb-118	3.86E-41
Cd-115m	3.20E-05	Tb-158	8.09E-11	Yb-169	4.63E-18	Y-87	6.69E-42
Co-60	2.91E-05	Sm-145	6.46E-11	Pm-143	3.25E-18	As-72	2.12E-42
Tb-160	2.33E-05	Gd-151	4.74E-11	Ca-45	2.81E-18	Se-72	1.81E-42
Zr-93	2.03E-05	Rh-101	4.45E-11	Tb-161	1.56E-18	Sb-122	1.01E-43
Eu-152	2.03E-05	Ho-166m	3.26E-11	Gd-152	1.40E-18		
Fe-59	1.15E-05	Sm-147	2.31E-11	Cd-113	4.25E-19		

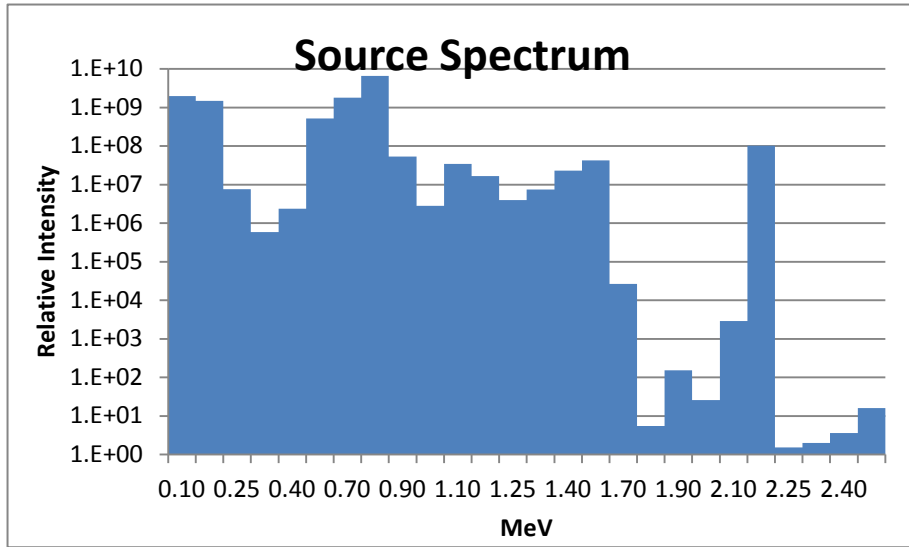


Figure 2-1. Semi-log plot of the combined photon spectrum.

Table 2-3. Intensity of gamma and X-ray components of the photon spectrum.

Top of energy bin, MeV	Gamma ray intensity	Bremsstrahlung x-ray intensity
0.10	1.96E+09	1.55E+04
0.20	1.47E+09	9.51E+03
0.25	7.56E+06	2.16E+03
0.30	5.86E+05	1.46E+03
0.40	2.36E+06	1.87E+03
0.60	5.19E+08	2.00E+03
0.70	1.81E+09	5.14E+02
0.80	6.57E+09	3.25E+02
0.90	5.39E+07	2.30E+02
1.00	2.79E+06	1.57E+02
1.10	3.47E+07	1.29E+02
1.20	1.66E+07	7.07E+01
1.25	3.95E+06	2.32E+01
1.30	7.41E+06	3.21E+01
1.40	2.33E+07	6.40E+01
1.60	4.28E+07	8.40E+01
1.70	2.66E+04	1.69E+01
1.80	3.82E-10	5.47E+00
1.90	1.48E+02	5.10E+00
2.00	8.04E+00	1.75E+01
2.10	2.87E+03	3.10E+00
2.20	1.03E+08	2.89E+00
2.25	1.23E+00	2.91E-01
2.30	1.38E+00	6.13E-01
2.40	3.59E+00	0.00E+00
2.60	1.50E+01	1.03E+00

The nuclides in Table 2-2 were compared to the RADDECAY tables, and a list of all photons and the associated probabilities was created. The probability was multiplied by the relative activity present for each nuclide to provide a probability for each photon energy. A histogram of 30 elements was created, representing 30 energy bins divided evenly between 0 and 3 MeV. For each bin, the total

probability of all photons within that bin was summed together to provide the relative probability for that energy range, essentially averaging the energy within the range.

Note that MCNP discards photons with energies below 0.015 MeV by default. Photons with energies at or below this level are stopped by the plastic cover over the film and do not contribute to the energy deposited in the film.

2.2 BREMSSTRAHLUNG PHOTONS

Bremsstrahlung X-ray photons are produced when the beta radiations from the nuclides present strike atoms in the wastes. The total activity from the beta-emitting nuclides in Table 2-2 was summed together to provide a beta source. An MCNP calculation was run with this source diffused evenly within the tank volume as described in Section 2.4 to provide the expected X-ray spectrum that would have resulted from the interaction of the beta particles in the chemistry of the sludge.

The bremsstrahlung X-ray spectrum, normalized by the fraction of total activity in the mixture, is included in the spectrum shown in Figure 2-1.

2.3 COMBINED GAMMA AND X-RAY PHOTON SPECTRUM

Figure 2-1 illustrates the combined gamma and bremsstrahlung X-ray components of the photon spectrum. The same data are listed in Table 2-3 above. Almost all of the spectral intensity of the photon source is due to the gamma ray component. The bremsstrahlung contribution is an important component for some of the lower-energy bins. The vertical scale indicates the relative flux for each energy bin.

2.4 MATHEMATICAL MODEL OF THE WORK ENVIRONMENT

The model describes workers on the “roof” above a below-grade Type III tank filled with a sludge-liquid mixture (Figure 2-2). The tank is 33 ft deep and 85 ft in diameter. Over the tank is a 4-ft layer of concrete (Bebbington 1990, p. 129). Penetrating the concrete are openings used for examination or for sampling the contents. The model included a 6-in.-radius port, filled with air extending through the concrete shielding to the surface to simulate one of these openings.

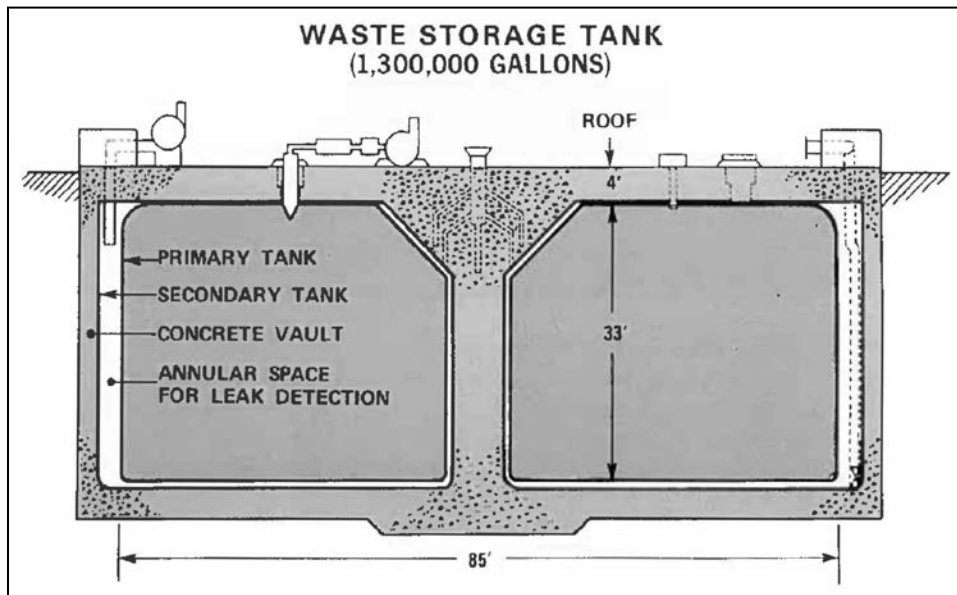


Figure 2-2. Cross-sectional diagram of a Type III tank.

The elemental composition of the sludge-liquid mixture was based on actual chemical sampling and contained significant amounts of aluminum, calcium, and iron in addition to many other elements (Pasala 2011, pp. 52–53, 55). For the model, the sludge and the liquid phase were mixed at a 70%:30% ratio, respectively, and were distributed evenly through the volume of the tank. In practice, the tanks were not full. Table 2-4 lists the relative abundance of the elements in the modeled tank. Other elements known to be present at much smaller concentrations were not included in the model.

Table 2-4. Tank contents — elements and relative abundances.

Relative abundance	Element
0.363615	O
0.24777	Na
0.139552	H
0.132923	K
0.076349	N
0.015899	Al
0.009262	Fe
0.008161	C
0.001907	S
0.001869	Mn
0.00133	Ca
0.000331	F
0.000268	Cl
0.000181	P
9.98E-05	Cu
9.90E-05	Cr
8.03E-05	Zn
7.22E-05	Mg
5.94E-05	Ag
3.79E-05	Ce
2.89E-05	Se
2.73E-05	Ba
2.33E-05	La
1.06E-05	Si
8.98E-06	Hg
5.24E-06	Cs
5.13E-06	Co
4.90E-06	As
4.83E-06	Nd
4.58E-06	Pb
3.11E-06	Sr
2.80E-06	Ra
1.73E-06	Zr
6.15E-07	Ni
1.75E-07	Cd

Workers were present atop the tanks performing their duties while standing or, in some instances, squatting or kneeling. Figure 2-3 is a photograph of such activity and includes an example of both a standing and a kneeling worker.

The workers were each modeled as a set of stacked cylinders based on the BOMAB phantom. This phantom was filled with a mixture of hydrogen, carbon, and oxygen to simulate the shielding and backscatter effect of a worker in the ambient field. The relative exposure at the abdomen or waist level and at the chest level was modeled for both a standing worker and a kneeling worker. For the standing worker, these points were approximated as 140 cm (55 in.) and 90 cm (35 in.) above the



Figure 2-3. SRS workers measuring the level of waste in a tank.

ground surface. For the kneeling worker, the points were 90 cm (35 in.) and at 40 cm (16 in.) above the ground surface.

In Figures 2-4 and 2-5, the worker models are shown on top of the tank. Circles at the chest and abdomen indicate the measurement points. In both figures the worker is shown near a 6-in.-radius opening that extends downward uninterrupted through the concrete shield to the sludge.

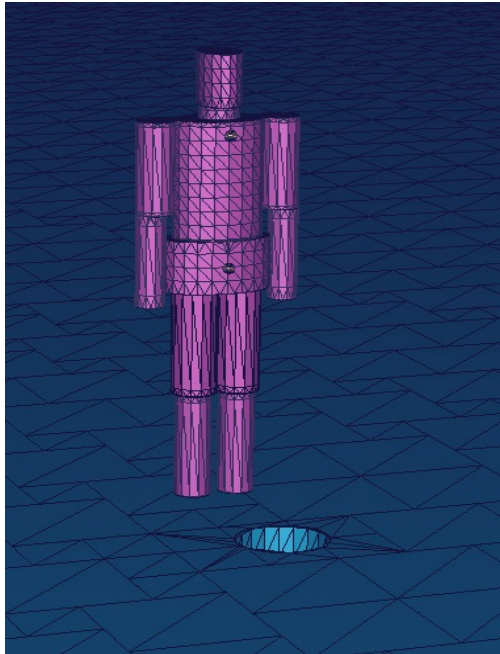


Figure 2-4. Model of standing worker.

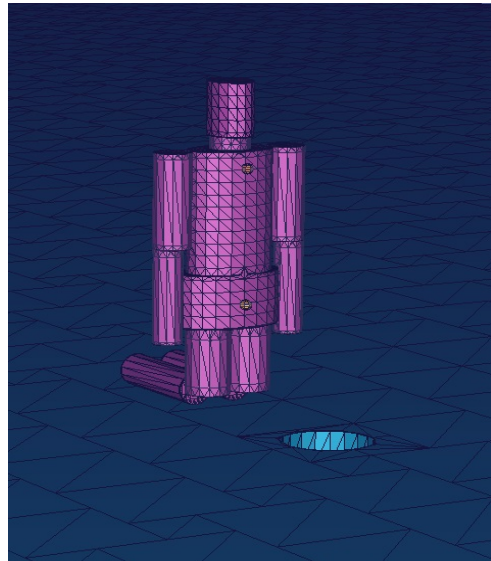


Figure 2-5. Model of kneeling worker.

This opening simulates the ports that were used for sample removal and for tank volume measurements, as in the pictures above. The lateral distance between the vertical plane of the measurement points and the center of the port is 50 cm (20 in.).

2.5 RESULTS

Four cases were examined: the standing worker near a port, the kneeling worker near a port, the standing worker without the port, and the kneeling worker without the port. In the latter two cases, the worker phantom was left in place and the opening was removed from the model. Results at the chest and abdomen locations for each of the four cases are graphed in Figures 2-6 through 2-9. These are the dose values plotted as a function of energy.

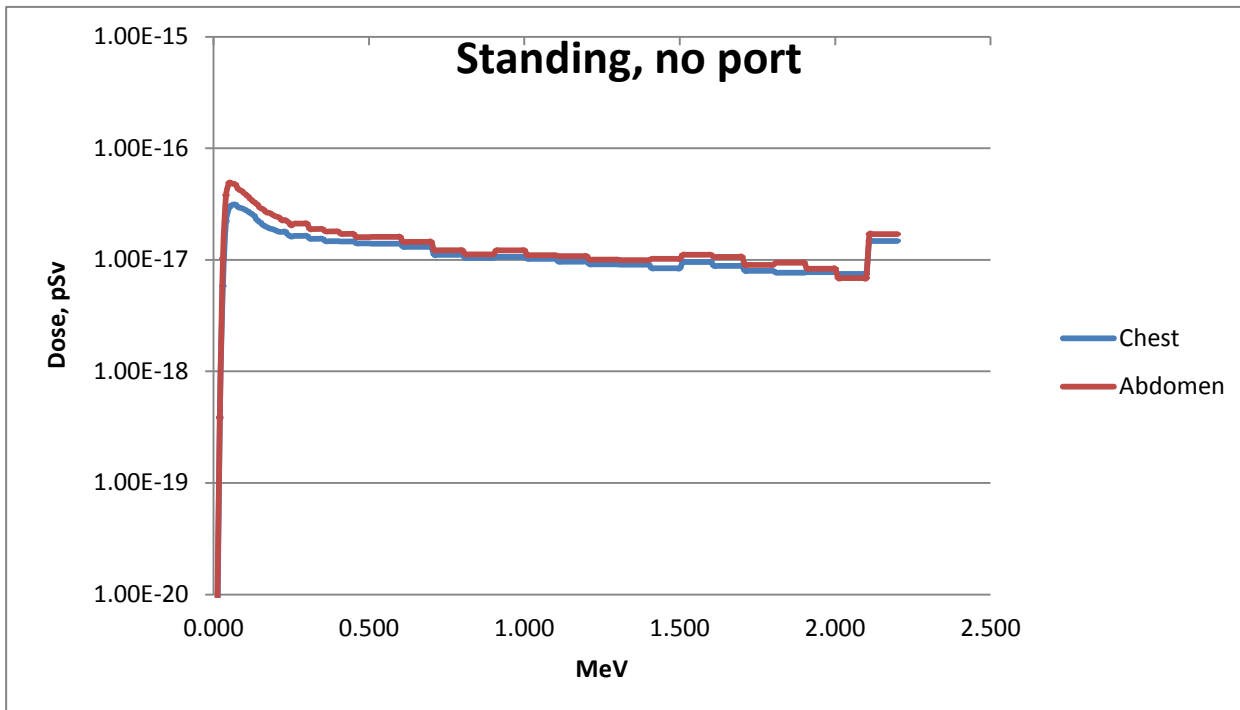


Figure 2-6. Standing worker, no port.

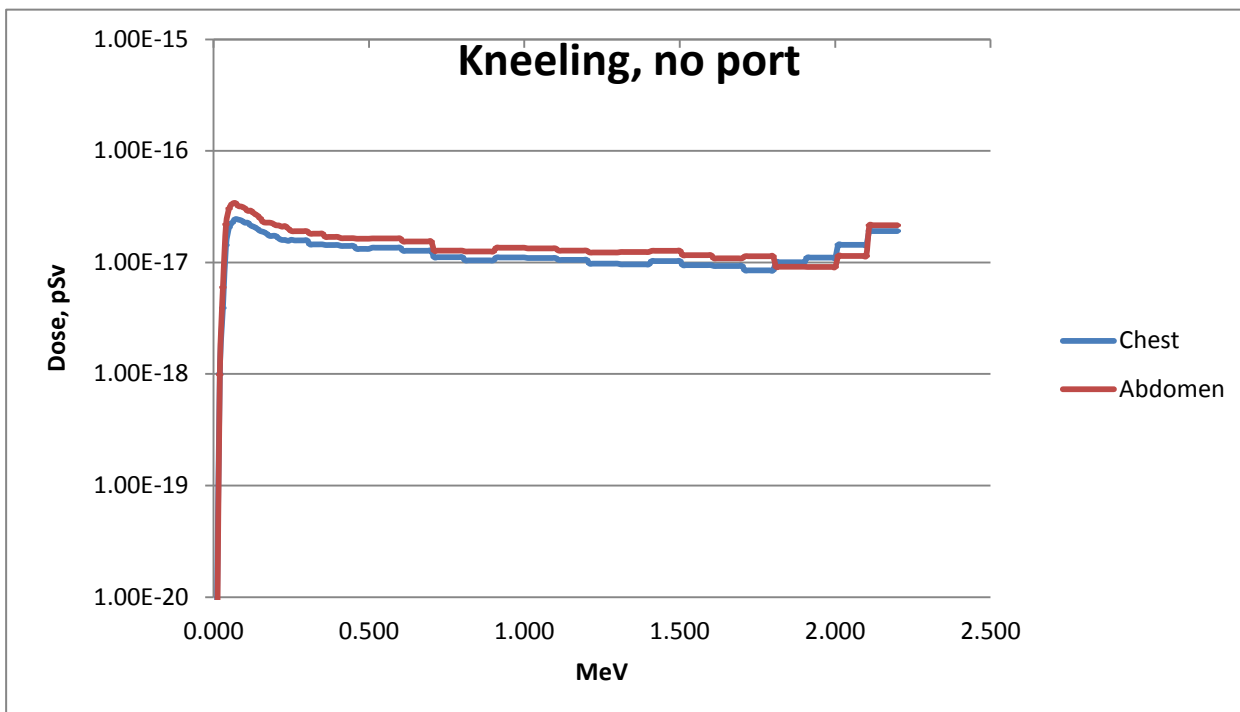


Figure 2-7. Kneeling worker, no port.

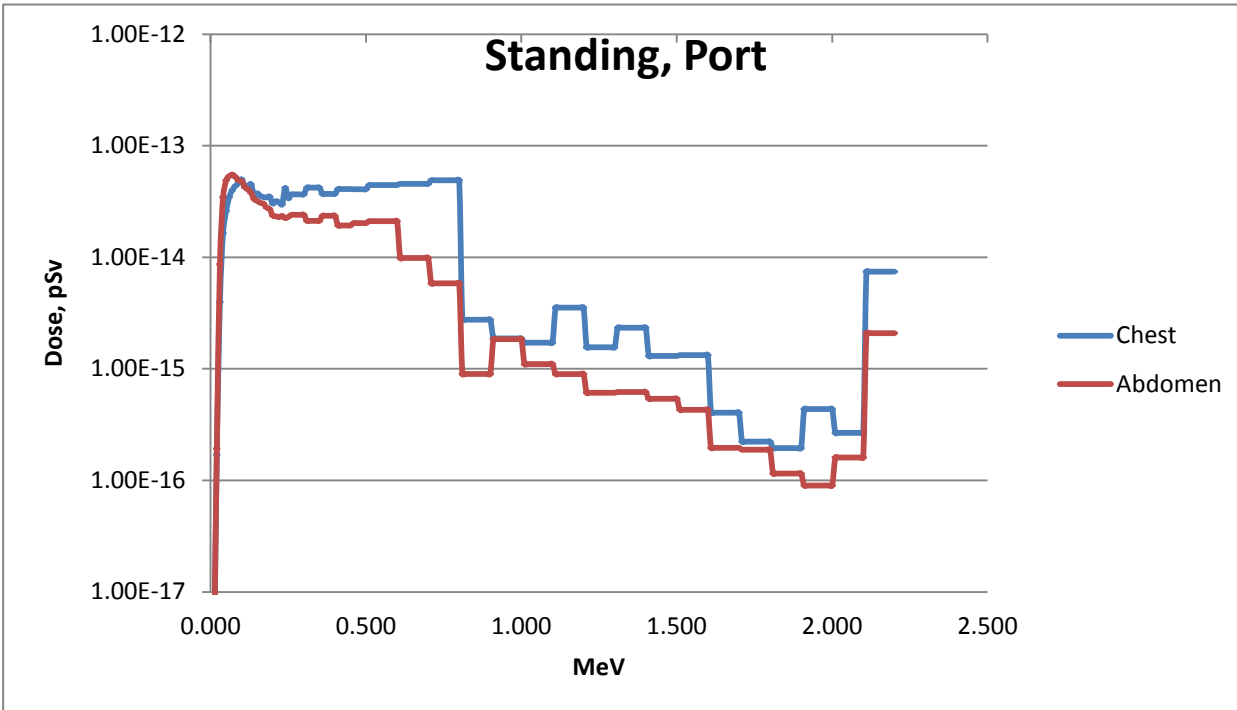


Figure 2-8. Standing worker, near a port.

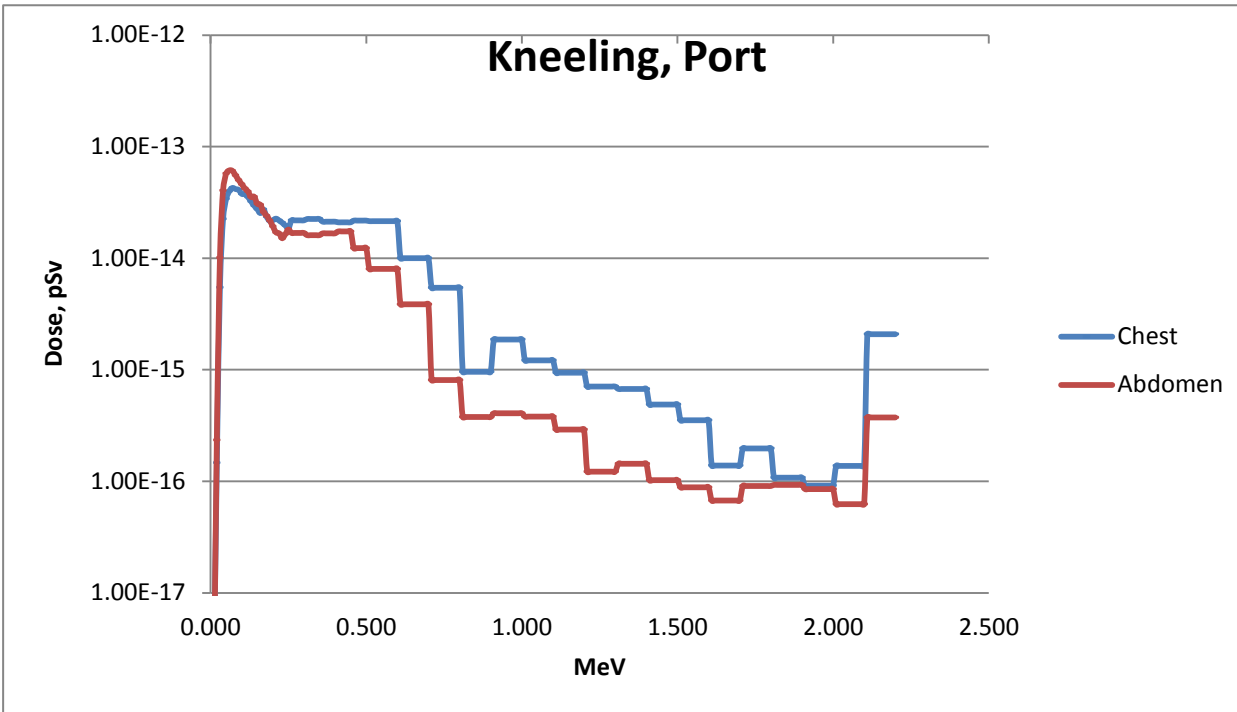


Figure 2-9. Kneeling worker, near a port.

At each measurement point, the total dose, the dose between 30 and 250 keV (Table 2-5), and the dose above 250 keV (Table 2-6) were measured. These were calculated using International Commission on Radiological Protection (ICRP) Publication 74 dose conversion factors (ICRP 1996) for results as $H_p(10,0^\circ)$ in picosieverts per source photon. For each, the chest result was divided by the abdomen result to obtain the dose to the abdomen relative to the dose at the chest. The contribution of the dose from the energy range less than 30 keV was much less than the total. For each of the four cases, the fraction of the dose from this range was less than 0.3%.

Table 2-5. Dose ratios for the 30- to 250-keV energy range.

Position	Chest	Abdomen	Ratio
Standing, no port	1.16×10^{-15}	1.67×10^{-15}	1.44
Kneeling, no port	9.48×10^{-16}	1.28×10^{-15}	1.35
Standing, port	1.73×10^{-12}	1.86×10^{-12}	1.08
Kneeling, port	1.51×10^{-12}	1.90×10^{-12}	1.26

Table 2-6. Dose ratios for the greater than 250-keV energy range.

Position	Chest	Abdomen	Ratio
Standing, no port	5.70×10^{-16}	6.58×10^{-16}	1.16
Kneeling, no port	5.90×10^{-16}	6.94×10^{-16}	1.18
Standing, port	1.05×10^{-12}	4.54×10^{-13}	0.43
Kneeling, port	4.53×10^{-13}	2.77×10^{-13}	0.61

For the cases where the worker was not near a port, all ratios indicate a higher exposure to the abdomen than to the chest where the film badge was worn. The highest ratio for the 30- to 250-keV range is 1.44. The highest ratio for the greater than 250 keV energy range is 1.18.

When a port was included in the model, the ratios are not as straightforward. For the lower energy range, the ratios indicate a higher exposure at the abdomen. However, doses from photons with energies greater than 250 keV are equal to or higher at the chest than at the abdomen. This is due to beaming effect of the open port. It was observed that the doses diminished with increasing height when measured directly over the port or when there was no port present. However, when measured at a short distance from a port, doses increased with increasing height in the greater than 250-keV range. This is apparently due to the beam created by the port spreading out laterally with increasing elevation. The highest ratio for the 30- to 250-keV range is 1.26. For the greater than 250-keV range, it is 0.61.

The values in Tables 2-5 and 2-6 show roughly a factor of 1,000 increase to the measurement points when the port was present. This indicates that the majority of photons came through the port. There is not a direct path from any of the measurement points to the sludge. All dose comes from photons either passing through the shield or scattered from the walls of the port. Photons that interact with matter and then result in a photon on a different path, "scattered" photons, undergo Compton scattering. The reversed ratios for the cases near the port are explained by two known effects of Compton scattering. The equations that describe this process indicate that the probability of the resultant path decreases with increased angle. That is, more photons scatter along a shallow angle than a large angle. Photons that scattered along the sides of the port underwent a shallower angle to reach the chest than the abdomen so there were more photons received at the chest. The second effect can be seen in the graphs for the port cases. In Compton scattering, the resultant photon has less energy than the originating photon. The energy decreases with increasing angle. Therefore, photons that scattered toward the abdomen had, on average, less energy than those that scattered toward the chest.

The model is based on the best estimate of radioactivity in the tanks and actual chemical constituent measurements within a tank. The tank dimensions and concrete thicknesses are modeled accurately according to the published information. However, there are two conservative assumptions built into this model that are favorable to claimants: (1) the tanks were modeled as filled to the top with an even mixture of the sludge and liquid phase, and (2) the port was filled with air for its entire length and had no cap.

For the first item, any increase in distance between the worker and the source should bring any ratio closer to 1. The sludge, which contained the greatest amount of the radioactivity, would have settled

to some degree within the liquid phase, and the top of the liquid would have been further away from the worker.

For the second item, any shielding in or over the port would reduce the streaming effect.

To obtain ratios that may be used to split total dose to the fraction that is between 30 and 250 keV and the fraction that is greater than 250 keV, the above data in Tables 2-5 and 2-6 may be used. It is assumed that the total dose is a sum of the two regions. The fraction for each region for the chest results are shown in Table 2-7. The chest location is used as the badge is presumed to have been worn at the chest.

Table 2-7. The fractions of total dose by energy range for each scenario.

Position	30–250 keV	>250 keV
Standing, no port	67%	33%
Kneeling, no port	62%	38%
Standing port	62%	38%
Kneeling port	77%	23%

As the greatest exposure to workers atop the tanks would be from work near an open port, the open port scenarios are averaged together to obtain a 70% fraction for the 30 to 250 keV range and 30% for the range greater than 250 keV.

These factors are independent of the above dose ratios and would be applied prior to their use. For example, a total dose of 100 millirem could be fractioned into 70 millirem for the 30 to 250 keV range and 30 millirem for the greater than 250 keV range. The 70 millirem would then be multiplied by an adjustment factor based on the limiting ratio in Table 2-5. The same process would apply to the 30 millirem fraction based on the factor based on the limiting ratio in Table 2-6.

2.6 GLOVEBAG DATA

Survey forms from the SRS for work on top of tanks in the tank farm contain a few survey readings that were taken during actual operations. Although these are from recent years, these are included as a verification of the modeling process (WSRC 2006a, 2006b).

Surveys were done in conjunction with sampling of the tank contents. A glovebag was assembled over the open sampling hole and samples were withdrawn into this controlled area (Figure 2-10). Survey readings were taken over the open hole and over and around the glovebag after its assembly. These readings were recorded as millirem per hour.

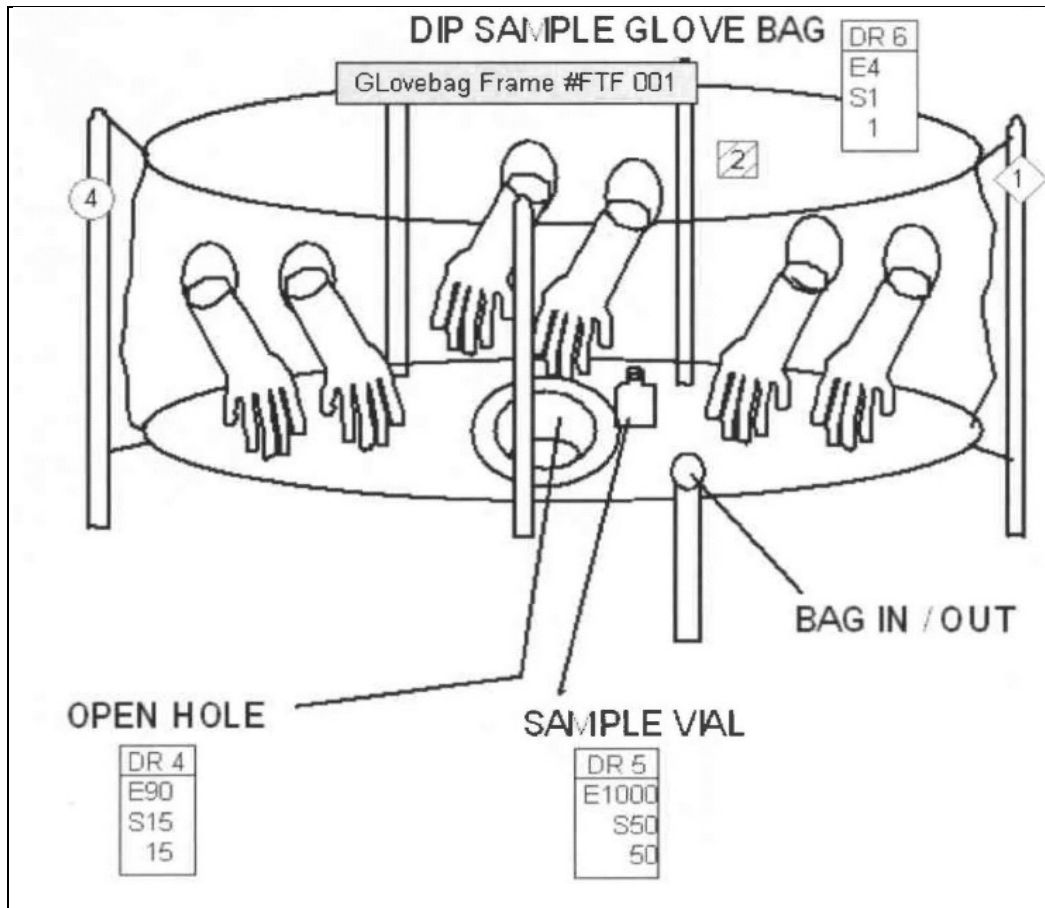


Figure 2-10. Diagram of glovebag and reading locations.

The survey forms contained a diagram of the glovebag arrangement and survey locations. Direct reading measurements were indicated as "DR". Note that in Figure 2-10, are the location of the open hole readings and for location 2. In the document location 2 readings were labeled as "top of glovebag" (WSRC 2006b).

Readings labeled "over open hole" were paired with readings labeled "top of glovebag" and ratios were calculated (WSRC 2006a, 2006b, 2006c). These readings are listed in Table 2-8. The ratios ranged from 10 to 70 for the whole-body results. Note that there is no indication in these documents that workers worked directly over these open holes; rather, they were positioned to one side.

Table 2-8. Survey readings taken above ports on SRS tanks.

Open Hole mrem/hr	Top of glovebag mrem/hr	Ratio
15	1	15
15	1	15
10	1	10
350	5	70

Using the open port model, points were measured in the vertical centerline over the open port. The 80 centimeter value was compared to the value directly over the hole to obtain a ratio of 10. The 215 centimeter value provided a ratio of 90.

In Figure 2-11, the ratios obtained from the survey forms and the ratios calculated from MCNP are shown with an approximation of their distances above the open port. These are based on an assumption that the top of the glovebag is 20 inches from the base. The documents do not state the height of the glovebag.

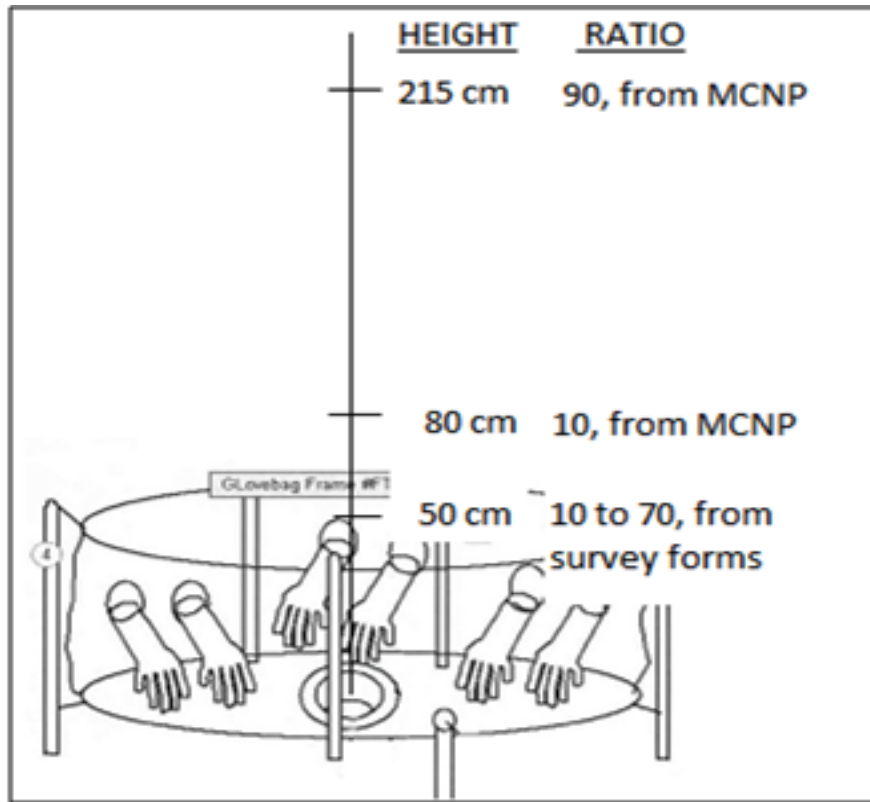


Figure 2-11. Ratios from Survey Forms and MCNP calculations.

Although the ratios from the actual measurements do not match exactly for the distances involved, they are well within the expected range and can therefore be considered a verification of the process.

2.7 MATHEMATICAL MODEL OF THE DOSIMETER

The SRS dosimeter is described by Richardson, Wing, and Daniels (2006) and Taulbee (2009). Taulbee's MCNP dosimeter model was intended to register neutron dose and included nuclear track emulsion, type A (NTA) film. For this photon dose analysis, the NTA film in Taulbee's MCNP dosimeter model was replaced with DuPont Type 555 film. DuPont films (predominantly Type 555 and at times Type 55x) were used in the SRS dosimeter (Wells 2000). Figure 2-12 is an exploded view of the film badge model.

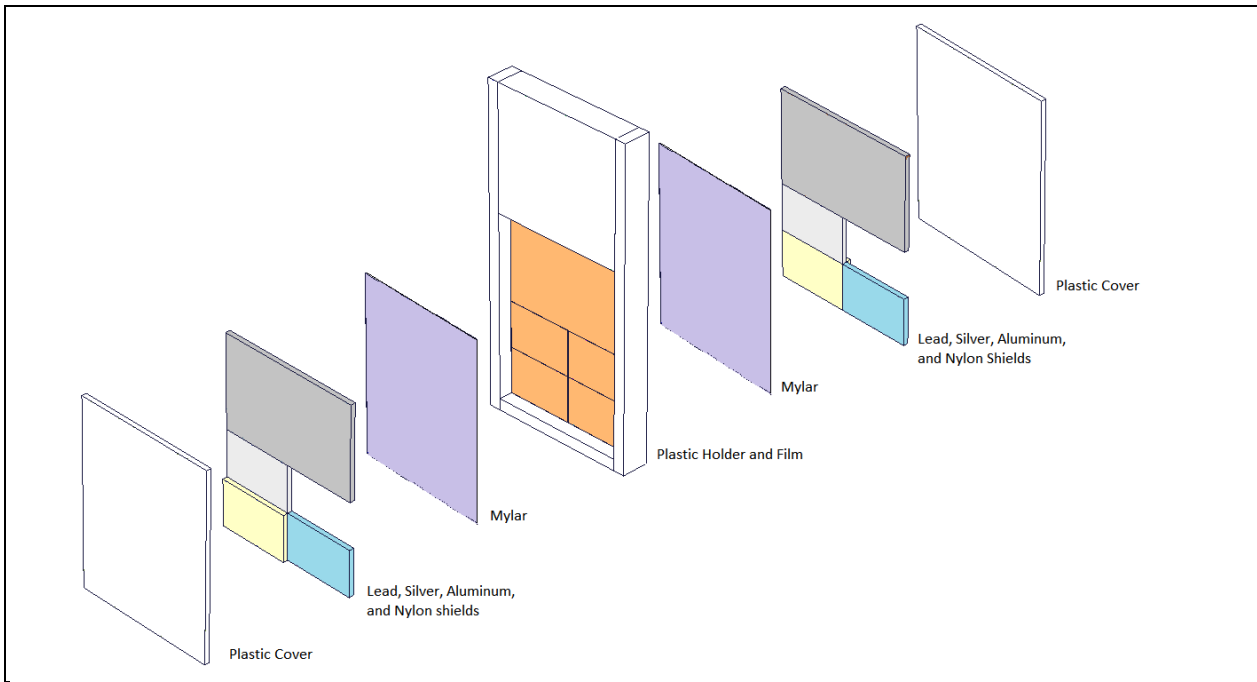


Figure 2-12. Exploded view of SRS film badge model.

Five different portions of the film, each with different coverings or “filters” were tallied. Each portion of the film had the same filtration in front and back of the film:

- Upper portion of the film covered front and back by 1 mm of lead,
- Open window (OW) region covered by no filter (other than the thin Mylar light enclosure and surrounding plastic cover),
- Portion of the film covered front and back by 1 mm of silver,
- Portion covered front and back by 2 mm of aluminum, and
- Portion filtered covered front and back by 1 mm of nylon plastic.

In this analysis, only the energy deposition in the OW and silver filter portions of the film are important. The OW film was used to define the penetrating plus nonpenetrating dose, while the silver filter film defined the penetrating dose. The other portions of the film were not routinely analyzed (Richardson, Wing, and Daniels 2006).

A planar source was placed immediately in front of the badge and constrained to provide photons traveling toward the film perpendicular to the film plane. Behind the film was modeled a rectangular solid 15 cm thick, 30 cm tall, and 30 cm wide and filled with the same material as the worker phantom to provide realistic backscatter to the film badge as it was worn.

2.8 DOSIMETER RESPONSE

Fundamental to this problem was the selection of the correct MCNP tally type to represent the quantity of interest. The beginning assumption was that a tally designed to register the energy deposition in the cell representing the film was appropriate. This would be either an *F4 tally or the F6 tally. The *F4 tally is reported in units of megaelectron-volts per square centimeter, and the F6 tally is in units of megaelectron-volts per gram. The F6 tally includes a microscopic total cross section in its

computation. A simple simulation was run to select a tally that reacts proportionally to optical density observed in the exposed film.

It is well known that dosimeter film has a nonlinear response with photon energy as shown on the OW line on the left hand side of Figure 2-13, which was taken from Figure A-1 of ORAUT-OTIB-0010, *A Standard Complex-Wide Methodology for Overestimating External Doses Measured with Film Badge Dosimeters* (ORAUT 2006). The natural logarithm of the actual responses was used for Figure 2-13, and the magnitude of the MCNP values is smaller. The simulation measured the response of a sphere of unshielded Kodak Type AA dosimeter film around a point source of monoenergetic photons. The photon energy was varied, and both the *F4 and F6 tally results were obtained. The *F4 tally displayed a linear response. The F6 tally showed a nonlinear response with a peak at the same energy as the Kodak Type AA film. This confirmed that the F6 tally is appropriate to represent energy deposited in the film. For reporting purposes, the F6 tally result is multiplied by 1.603×10^{-10} to convert from megaelectron-volts per gram per source photon to gray per source photon.

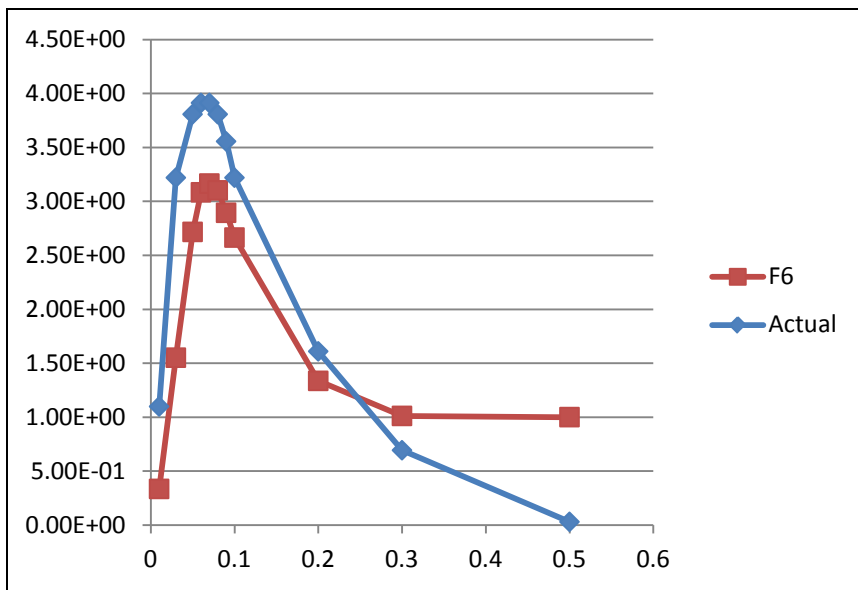


Figure 2-13. Comparison of the actual curve of two-element film dosimeter OW response (ORAUT 2006) to an MCNP simulation. Similarity of shape confirms that the F6 tally is appropriate.

As the film thickness is 38 microns, the film badge models tallied the total energy deposited from electrons rather than from the incident photons. For an F6 photon tally, MCNP calculates the energy deposited within a volume as the energy left by the photon. Some of that energy may subsequently escape if the electron path length is significant relative to the volume size. However, the electron energy may be tallied instead to account for this effect. When using an F6 electron tally, MCNP measures only the energy deposited within the volume only for the portion of the electron path within the volume, providing a more accurate estimate of the energy imparted to the thin film.

To create the energies that would be seen by the film badge, a histogram energy spectrum was created for each of the measurement points (the chest and abdomen locations) of the standing and kneeling workers for both of the “port” and “no port” cases, a total of eight full spectra. Each spectrum was created from information captured by MCNP at each measurement point tallying the number of photons within select energy bands. These bands were divided into 10-keV bands between 0 and 250 keV, 50-keV bands up to 500 keV, and 100-keV bands above 500 keV. The lower energies were more finely divided to create ranges appropriate for the film’s response curve. The spectrum was created as a histogram of these energy regions with the value of each the relative flux of photons within that range.

Data used to create these spectra are listed in Attachment A. The film badge model was run in MCNP using each of these spectra as a description of the source of photon radiation. The film badge model was run with each spectrum for each of the eight measurement locations.

The energy deposited in each area within the film was calculated. Ratios of the chest and abdomen location results were calculated to assess the relative film response of a badge that would have been in the abdomen area to a badge that would have been at the chest. Note that this does not include the relative intensities of the radiation fields at those locations, only the relative response of the film badge to the spectra estimated to have been present at those locations. The MCNP results that formed the basis of the ratios were calculated on a per-photon basis, normalizing each spectrum.

Because the greatest majority of the dose was in the region greater than 30 keV, and the silver-shielded area would have been used for the penetrating exposure results, the relative response of film to the chest and abdomen spectra was calculated. Table 2-9 lists the ratios that were obtained for the silver-shielded area of the film.

Table 2-9. Silver-shielded film ratios.

Position	Ratio
Standing, no port	1.00
Kneeling, no port	1.02
Standing, port	1.05
Kneeling, port	1.03

These ratios indicate that the film response was most similar between the chest and abdomen locations when there was no port present. The relative response was greater at the chest location than would have been seen if the dosimeter was placed at the abdomen location for the cases when a port was present. This can be explained by the resultant energy of the scattered photons when a port was present, as explained in Section 2-5, above. Photons that were scattered toward the abdomen, had on average, less energy than those scattered toward the chest.

3.0 SUMMARY

For routine work in radiological areas, radiation workers are normally instructed to wear their dosimeter at a location on the front of the torso between the collar and belt. The difference in dosimeter response to the penetrating photon spectrum in the SRS tank farms that is attributable to dosimeter placement was modeled using MCNP. The model produced the following results:

- The contribution to the total dose from the dose in the range from 0 to 30 keV is less than 0.3%.
- The photon flux drops as the elevation increases for areas away from tank penetrations.
- The photon flux increases as the elevation increases for areas near tank penetrations.
- For dosimetry at a site in the abdomen when the badge was worn at the collar, the badge dose should be adjusted upward by a factor of 1.44. The relative response at the chest in comparison with the waist of the film badge component used for penetrating exposure is 0.43 to 1.18 for photon energies encountered over the tank.
- A total dose result may be fractioned into two doses; 70% of the dose may be assumed to have been in the 30 to 250 keV range and 30% in the greater than 250 keV range.

- The modeled response of the silver-shielded film in the calculated spectra indicates a ratio of 1.05 for workers near a port and 1.02 for workers not near a port.
- These factors are based only on the geometry of working over a tank at the SRS Tank Farm and are independent of all other modifying factors.

4.0 ORGAN DOSE CONVERSION FACTORS

Chen (1991) performed detailed analyses of the effective beam beam orientation from an underfoot infinite planar source and resulting radiation doses. From the analyses, Chen concluded that the rotational (ROT) beam geometry provided the most realistic organ dose conversion factors. Chen also reported the anterior-posterior (AP) geometry resulted in dose conversion factors that exceeded those using ROT by as much as a factor of 2. Eckerman and Ryman (1993) independently verified that dose equivalents based on the ROT geometry were in excellent comparison to dose equivalents reported by Chen.

To be favorable to claimants, the National Institute for Occupational Safety and Health (NIOSH) has stated that dose conversion factors using the AP geometry when the dosimeter was worn on the chest does not result in underestimation of dose with the exception of four organs; those are bone surface, bone red marrow, esophagus, and lung. In the case of these four organs, dose conversion factors for the ROT geometry should be used. AP and ROT dose conversion factors are provided in Appendix A of OCAS-IG-001, *External Dose Reconstruction Implementation Guideline* (NIOSH 2007). ROT dose conversion factors should also be multiplied by the appropriate energy range correction factors in Table 4.1a of NIOSH (2007).

5.0 CONCLUSIONS

It is reasonable to expect that a common exposure scenario in the SRS tank farm was one involving a worker standing over a tank in a normal posture and working near a tank opening. It is favorable to claimants to apply the adjustment factors to all workers who were associated with tank farm operations. Total dose results may be fractioned into a 70% component in the 30 to 250 keV range and 30% for the greater than 250 keV range. An adjustment factor of 1.5 is recommended for doses in the 30 to 250 keV range and a factor of 1.2 for doses in the greater than 250 keV range. These are rounded upward to account for the film badge response and to be claimant favorable.

REFERENCES

- Bebbington, W. P., 1990, *History of Du Pont at the Savannah River Plant*, E. I. du Pont de Nemours and Company, Wilmington, Delaware. [SRDB Ref ID: 11249]
- Chen, S. Y., 1991, "Calculation of Effective Dose-Equivalent Responses for External Exposure from Residual Photon Emitters in Soil," *Health Physics*, volume 60, number 3, pp. 411–426.
- Eckerman, K. F., and J. C. Ryman, 1993, *External Exposure to Radionuclides in Air, Water, and Soil*, Federal Guidance Report No. 12, EPA-402-R-93-081, U. S. Environmental Protection Agency, Office of Radiation and Indoor Air, Washington, D.C., September. [SRDB Ref ID: 11997]
- ICRP (International Commission on Radiological Protection), 1996, *Conversion Coefficients for Use in Radiological Protection Against External Radiation*, Publication 74, Pergamon Press, Oxford, England.
- Kocher, D. C., 1981, *Radioactive Decay Data Tables, A Handbook of Decay Data for Application to Radiation Dosimetry and Radiological Assessments*, DOE/TIC-11026, U.S. Department of Energy, Technical Information Center, Oak Ridge, Tennessee, April. [SRDB Ref ID: 32563]
- NIOSH (National Institute for Occupational Health and Safety), 2007, *External Dose Reconstruction Implementation Guideline*, OCAS-IG-001, Rev. 03, Cincinnati, Ohio, November 21.
- ORAUT (Oak Ridge Associated Universities Team), 2006, A Standard Complex-Wide Methodology for Overestimating External Doses Measured with Film Badge Dosimeters, ORAUT-OTIB-0010, Rev. 01, Oak Ridge, Tennessee, June 5.
- Pasala, N. R., 2011, Information on the Radiological and Chemical Characterization of the Savannah River Site Tank Waste, As of July 5, 2011, SRR-LWE-2011-00201, Rev. 0, Savannah River Remediation, Savannah River Site, Aiken, South Carolina, September 26. [SRDB Ref ID: 111851]
- Richardson, D. B., S. Wing, and R. D. Daniels, 2006, "Evaluation of External Radiation Dosimetry Records at the Savannah River Site, 1951–1989," *Journal of Exposure Science and Environmental Epidemiology*, volume 17, pp. 13–24. [SRDB Ref ID: 46009]
- Taulbee, T. D., 2009, *Measurement and Model Prediction of Proton-Recoil Track Length Distributions in NTA Film Dosimeters for Neutron Energy Spectroscopy and Retrospective Dose Assessment*, University of Cincinnati, Cincinnati, Ohio, March. [SRDB Ref ID: 118570]
- Wells, D. W., 2000, "Advances in External Dosimetry at the Savannah River Site," p. 247, *Proceedings of the Symposium, May 17, 2000, 50 Years of Excellence in Science and Engineering at SRS*, WSRC-MS-2000-00061, Westinghouse Savannah River Company, Aiken, South Carolina. [SRDB Ref ID: 46147]
- WSRC (Westinghouse Savannah River Company), 2006a, *Tank 32 H-Riser Dip Samples*, Survey TKFM-M-20060410-14, Savannah River Site, Aiken, South Carolina, April 11. [SRDB Ref ID: 108763]
- WSRC (Westinghouse Savannah River Company), 2006b, *Dip Samples @ Tank 47*, Survey TKFM-M-20060224-4, Savannah River Site, Aiken, South Carolina, February 25. [SRDB Ref ID: 108720]

WSRC (Westinghouse Savannah River Company), 2006c, *Tank 43 G-Riser Dip Sampling, Survey TKFM-M-20060403-9, Savannah River Site, Aiken, South Carolina, April 3.* [SRDB Ref ID: 108762]

ATTACHMENT A
ENERGY SPECTRA CALCULATED FROM TANK MODELS FOR FILM BADGE MODELS
Page 1 of 4

Table A-1. Standing worker, no port, 140 and 90 cm.

Standing, Port, 140 cm			Standing, Port, 90 cm		
Energy	Result	Relative error	Energy	Result	Relative error
0.010	1.61E-20	0.38	0.010	4.29E-20	0.49
0.020	3.70E-19	0.35	0.020	3.62E-19	0.25
0.030	7.18E-18	0.04	0.030	1.27E-17	0.04
0.040	3.46E-17	0.03	0.040	5.92E-17	0.03
0.050	5.32E-17	0.02	0.050	8.88E-17	0.03
0.060	6.11E-17	0.02	0.060	9.42E-17	0.02
0.070	6.03E-17	0.02	0.070	9.10E-17	0.03
0.080	5.59E-17	0.02	0.080	8.09E-17	0.02
0.090	5.11E-17	0.02	0.090	7.26E-17	0.03
0.100	4.64E-17	0.02	0.100	6.41E-17	0.03
0.110	4.09E-17	0.02	0.110	5.57E-17	0.03
0.120	3.61E-17	0.02	0.120	4.81E-17	0.03
0.130	3.21E-17	0.02	0.130	4.23E-17	0.03
0.140	2.73E-17	0.02	0.140	3.76E-17	0.03
0.150	2.44E-17	0.02	0.150	3.27E-17	0.03
0.160	2.15E-17	0.02	0.160	2.97E-17	0.03
0.170	1.95E-17	0.02	0.170	2.62E-17	0.03
0.180	1.78E-17	0.02	0.180	2.44E-17	0.03
0.190	1.66E-17	0.03	0.190	2.22E-17	0.03
0.200	1.53E-17	0.02	0.200	2.04E-17	0.03
0.210	1.42E-17	0.02	0.210	1.91E-17	0.03
0.220	1.35E-17	0.02	0.220	1.71E-17	0.03
0.230	1.30E-17	0.03	0.230	1.64E-17	0.03
0.240	1.17E-17	0.02	0.240	1.51E-17	0.03
0.250	1.08E-17	0.02	0.250	1.36E-17	0.03
0.300	4.56E-17	0.02	0.300	5.86E-17	0.03
0.350	3.70E-17	0.02	0.350	4.51E-17	0.03
0.400	3.10E-17	0.02	0.400	3.77E-17	0.03
0.450	2.76E-17	0.02	0.450	3.21E-17	0.03
0.500	2.40E-17	0.03	0.500	2.72E-17	0.03
0.600	4.07E-17	0.02	0.600	4.66E-17	0.03
0.700	3.35E-17	0.03	0.700	3.70E-17	0.04
0.800	2.84E-17	0.03	0.800	3.11E-17	0.04
0.900	2.41E-17	0.03	0.900	2.59E-17	0.05
1.000	2.05E-17	0.03	1.000	2.34E-17	0.05
1.100	1.85E-17	0.04	1.100	1.98E-17	0.05
1.200	1.64E-17	0.04	1.200	1.83E-17	0.06
1.300	1.47E-17	0.05	1.300	1.61E-17	0.07
1.400	1.38E-17	0.06	1.400	1.51E-17	0.08
1.500	1.22E-17	0.07	1.500	1.48E-17	0.10
1.600	1.32E-17	0.10	1.600	1.53E-17	0.14
1.700	1.17E-17	0.11	1.700	1.40E-17	0.13
1.800	1.01E-17	0.10	1.800	1.14E-17	0.12
1.900	9.31E-18	0.15	1.900	1.14E-17	0.14
2.000	9.04E-18	0.13	2.000	9.66E-18	0.17
2.100	8.47E-18	0.19	2.100	7.74E-18	0.17
2.200	1.62E-17	0.04	2.200	1.87E-17	0.06

ATTACHMENT A
ENERGY SPECTRA CALCULATED FROM TANK MODELS FOR FILM BADGE MODELS
 Page 2 of 4

Table A-2. Kneeling worker, no port, 90 and 40 cm.

Kneeling, No port, 90 cm			Kneeling, No port, 40 cm		
Energy	Result	Relative error	Energy	Result	Relative error
0.010	7.09E-20	0.43	0.010	2.07E-20	0.43
0.020	9.56E-19	0.51	0.020	9.37E-19	0.45
0.030	4.82E-18	0.09	0.030	7.37E-18	0.08
0.040	2.23E-17	0.06	0.040	3.42E-17	0.05
0.050	3.76E-17	0.04	0.050	5.52E-17	0.05
0.060	4.46E-17	0.03	0.060	6.55E-17	0.05
0.070	4.70E-17	0.03	0.070	6.54E-17	0.05
0.080	4.57E-17	0.04	0.080	6.03E-17	0.05
0.090	4.17E-17	0.03	0.090	5.54E-17	0.05
0.100	3.73E-17	0.03	0.100	5.01E-17	0.05
0.110	3.41E-17	0.03	0.110	4.34E-17	0.05
0.120	2.97E-17	0.03	0.120	4.02E-17	0.05
0.130	2.68E-17	0.03	0.130	3.53E-17	0.05
0.140	2.41E-17	0.03	0.140	3.16E-17	0.05
0.150	2.15E-17	0.03	0.150	2.79E-17	0.05
0.160	1.98E-17	0.03	0.160	2.41E-17	0.05
0.170	1.79E-17	0.03	0.170	2.24E-17	0.05
0.180	1.61E-17	0.04	0.180	2.11E-17	0.06
0.190	1.52E-17	0.03	0.190	1.96E-17	0.05
0.200	1.44E-17	0.04	0.200	1.79E-17	0.06
0.210	1.30E-17	0.03	0.210	1.70E-17	0.06
0.220	1.21E-17	0.04	0.220	1.58E-17	0.06
0.230	1.15E-17	0.04	0.230	1.53E-17	0.06
0.240	1.08E-17	0.04	0.240	1.40E-17	0.06
0.250	1.07E-17	0.05	0.250	1.27E-17	0.06
0.300	4.38E-17	0.03	0.300	5.28E-17	0.06
0.350	3.48E-17	0.03	0.350	4.32E-17	0.06
0.400	3.01E-17	0.03	0.400	3.55E-17	0.06
0.450	2.65E-17	0.03	0.450	3.10E-17	0.06
0.500	2.26E-17	0.03	0.500	2.78E-17	0.06
0.600	3.95E-17	0.03	0.600	4.76E-17	0.06
0.700	3.26E-17	0.04	0.700	3.93E-17	0.06
0.800	2.85E-17	0.04	0.800	3.26E-17	0.07
0.900	2.42E-17	0.04	0.900	2.90E-17	0.07
1.000	2.13E-17	0.05	1.000	2.60E-17	0.08
1.100	1.98E-17	0.06	1.100	2.41E-17	0.09
1.200	1.79E-17	0.07	1.200	2.17E-17	0.10
1.300	1.57E-17	0.08	1.300	1.97E-17	0.11
1.400	1.47E-17	0.09	1.400	1.89E-17	0.12
1.500	1.49E-17	0.10	1.500	1.84E-17	0.15
1.600	1.31E-17	0.12	1.600	1.60E-17	0.14
1.700	1.23E-17	0.12	1.700	1.43E-17	0.15
1.800	1.07E-17	0.14	1.800	1.43E-17	0.17
1.900	1.22E-17	0.20	1.900	1.11E-17	0.17
2.000	1.29E-17	0.22	2.000	1.06E-17	0.20
2.100	1.63E-17	0.25	2.100	1.29E-17	0.26
2.200	2.10E-17	0.10	2.200	2.36E-17	0.09

ATTACHMENT A
ENERGY SPECTRA CALCULATED FROM TANK MODELS FOR FILM BADGE MODELS
 Page 3 of 4

Table A-3. Standing worker, near port, 140 and 90 cm.

Standing, Port, 140 cm			Standing, Port, 90 cm		
Energy	Result	Relative error	Energy	Result	Relative error
0.010	2.08E-17	0.18	0.010	2.41E-17	0.32
0.020	1.62E-16	0.12	0.020	1.83E-16	0.14
0.030	4.89E-15	0.04	0.030	1.07E-14	0.03
0.040	2.57E-14	0.04	0.040	5.38E-14	0.03
0.050	4.72E-14	0.04	0.050	8.88E-14	0.03
0.060	6.81E-14	0.04	0.060	1.04E-13	0.03
0.070	7.70E-14	0.03	0.070	1.06E-13	0.03
0.080	8.22E-14	0.05	0.080	9.87E-14	0.03
0.090	8.09E-14	0.05	0.090	8.56E-14	0.03
0.100	8.19E-14	0.07	0.100	7.87E-14	0.05
0.110	6.39E-14	0.04	0.110	6.40E-14	0.03
0.120	6.06E-14	0.04	0.120	5.59E-14	0.03
0.130	5.80E-14	0.11	0.130	4.86E-14	0.04
0.140	4.28E-14	0.05	0.140	3.98E-14	0.04
0.150	4.20E-14	0.06	0.150	3.59E-14	0.04
0.160	3.73E-14	0.06	0.160	3.23E-14	0.04
0.170	3.41E-14	0.05	0.170	2.97E-14	0.04
0.180	3.19E-14	0.05	0.180	2.59E-14	0.04
0.190	3.07E-14	0.07	0.190	2.37E-14	0.06
0.200	2.52E-14	0.05	0.200	1.97E-14	0.04
0.210	2.53E-14	0.08	0.210	1.85E-14	0.05
0.220	2.36E-14	0.06	0.220	1.73E-14	0.06
0.230	2.16E-14	0.06	0.230	1.70E-14	0.13
0.240	2.91E-14	0.13	0.240	1.56E-14	0.08
0.250	2.25E-14	0.08	0.250	1.53E-14	0.11
0.300	1.02E-13	0.07	0.300	6.66E-14	0.11
0.350	1.01E-13	0.17	0.350	5.07E-14	0.06
0.400	7.76E-14	0.05	0.400	4.94E-14	0.08
0.450	7.69E-14	0.06	0.450	3.62E-14	0.06
0.500	6.94E-14	0.05	0.500	3.45E-14	0.05
0.600	1.29E-13	0.04	0.600	6.12E-14	0.04
0.700	1.16E-13	0.07	0.700	2.52E-14	0.05
0.800	1.25E-13	0.03	0.800	1.49E-14	0.14
0.900	6.37E-15	0.21	0.900	2.08E-15	0.21
1.000	3.60E-15	0.23	1.000	3.54E-15	0.65
1.100	3.09E-15	0.19	1.100	1.99E-15	0.18
1.200	6.01E-15	0.38	1.200	1.52E-15	0.24
1.300	2.50E-15	0.31	1.300	9.80E-16	0.17
1.400	3.56E-15	0.18	1.400	9.44E-16	0.20
1.500	1.89E-15	0.11	1.500	7.80E-16	0.15
1.600	1.83E-15	0.10	1.600	5.92E-16	0.21
1.700	5.33E-16	0.25	1.700	2.58E-16	0.38
1.800	2.80E-16	0.23	1.800	2.38E-16	0.31
1.900	2.35E-16	0.35	1.900	1.39E-16	0.26
2.000	5.06E-16	0.45	2.000	1.05E-16	0.20
2.100	3.01E-16	0.46	2.100	1.81E-16	0.26
2.200	8.16E-15	0.04	2.200	2.29E-15	0.03

ATTACHMENT A
ENERGY SPECTRA CALCULATED FROM TANK MODELS FOR FILM BADGE MODELS
Page 4 of 4

Table A-4. Kneeling worker, near port, 90 and 40 cm.

Kneeling, Port, 90 cm			Kneeling, Port, 40 cm		
Energy	Result	Relative error	Energy	Result	Relative error
0.010	2.17E-17	0.24	0.010	1.58E-17	0.19
0.020	1.40E-16	0.11	0.020	2.23E-16	0.37
0.030	6.74E-15	0.03	0.030	1.25E-14	0.04
0.040	3.51E-14	0.04	0.040	6.31E-14	0.04
0.050	6.19E-14	0.04	0.050	1.04E-13	0.04
0.060	7.81E-14	0.04	0.060	1.20E-13	0.04
0.070	8.21E-14	0.04	0.070	1.16E-13	0.04
0.080	7.87E-14	0.03	0.080	1.04E-13	0.04
0.090	7.19E-14	0.04	0.090	8.78E-14	0.04
0.100	6.19E-14	0.03	0.100	7.54E-14	0.04
0.110	5.62E-14	0.04	0.110	6.33E-14	0.04
0.120	4.90E-14	0.04	0.120	5.48E-14	0.04
0.130	4.15E-14	0.04	0.130	4.53E-14	0.04
0.140	3.54E-14	0.05	0.140	4.26E-14	0.10
0.150	3.09E-14	0.07	0.150	3.45E-14	0.04
0.160	2.66E-14	0.03	0.160	3.16E-14	0.06
0.170	2.70E-14	0.08	0.170	2.55E-14	0.04
0.180	2.19E-14	0.04	0.180	2.23E-14	0.04
0.190	1.90E-14	0.04	0.190	1.91E-14	0.06
0.200	1.82E-14	0.06	0.200	1.61E-14	0.05
0.210	1.80E-14	0.08	0.210	1.35E-14	0.05
0.220	1.65E-14	0.07	0.220	1.26E-14	0.07
0.230	1.51E-14	0.06	0.230	1.09E-14	0.06
0.240	1.37E-14	0.06	0.240	1.14E-14	0.09
0.250	1.24E-14	0.06	0.250	1.20E-14	0.12
0.300	6.07E-14	0.05	0.300	4.67E-14	0.08
0.350	5.38E-14	0.10	0.350	3.84E-14	0.10
0.400	4.47E-14	0.06	0.400	3.50E-14	0.08
0.450	3.95E-14	0.09	0.450	3.27E-14	0.07
0.500	3.71E-14	0.09	0.500	2.10E-14	0.07
0.600	6.25E-14	0.04	0.600	2.33E-14	0.11
0.700	2.56E-14	0.05	0.700	9.86E-15	0.21
0.800	1.39E-14	0.10	0.800	2.07E-15	0.10
0.900	2.22E-15	0.22	0.900	8.72E-16	0.16
1.000	3.59E-15	0.64	1.000	7.82E-16	0.19
1.100	2.19E-15	0.21	1.100	6.86E-16	0.37
1.200	1.60E-15	0.29	1.200	4.95E-16	0.35
1.300	1.14E-15	0.17	1.300	1.96E-16	0.12
1.400	1.03E-15	0.22	1.400	2.19E-16	0.26
1.500	7.08E-16	0.14	1.500	1.48E-16	0.16
1.600	4.88E-16	0.15	1.600	1.22E-16	0.11
1.700	1.83E-16	0.29	1.700	8.87E-17	0.14
1.800	2.49E-16	0.28	1.800	1.15E-16	0.26
1.900	1.31E-16	0.28	1.900	1.12E-16	0.30
2.000	1.06E-16	0.20	2.000	9.89E-17	0.19
2.100	1.56E-16	0.21	2.100	7.04E-17	0.22
2.200	2.29E-15	0.03	2.200	4.10E-16	0.04

ATTACHMENT B
DOSE MODELS
Page 1 of 35

Dose Model for a Standing Worker – No Port

SRS **Dosimeter** Ratio Worker on top of Type III Tank

C

C Roger Halsey - March 2013

C

C Film Badge Model from Robert Morris

C BOMAB Model from Tim Taulbee

C

C =====Cells=====

C

C BOMAB Phantom

120 208 -1.19 -80:-81:-82:-83:-84:-85:-86:-87:-88:-89:-90:-91 TRCL=3

C

C Air

163	101	-0.001205	-55	40.2	#120	
164	101	-0.001205	55	-56	40.2	#120
165	101	-0.001205	56	-57	-50	40.2
166	101	-0.001205	57	-58	-50	40.2
167	101	-0.001205	58	-59	-50	40.2
168	101	-0.001205	59	-50	40.2	

C

C Concrete

169	350	-2.3	-40	60	
170	350	-2.3	-40	-60	61
171	350	-2.3	-40	-61	62
172	350	-2.3	-40	-62	69
181	350	-2.3	-40	-69	70
182	350	-2.3	-40	-70	71
183	350	-2.3	-40	-71	72
184	350	-2.3	(-40	41	-72)

C

C Sludge

174 400 -1.23 -41

C

C Void

199 0 (50 40.2) : (-40.2 40)

C =====Surfaces=====

C

C BOMAB Phantom, Standing

80	rcc	-7.5	0	0	0	0	40	6	\$Right Calf
81	rcc	7.5	0	0	0	0	40	6	\$Left Calf
82	rcc	-7.5	0	40	0	0	40	7.5	\$Right Thigh
83	rcc	7.5	0	40	0	0	40	7.5	\$Left Thigh
84	rec	0	0	80	0	0	20	18	0 0 0 10 0 \$Pelvis
85	rec	0	0	100	0	0	45	15	0 0 0 10 0 \$Chest

ATTACHMENT B
DOSE MODELS
 Page 2 of 35

```

86      rcc   0   0   145   0   0   5   6.5          $Neck
87      rec   0   0   150   0   0   20  7   0   0   0   9.5 0   $Head
88      rcc -21.25 0   145   0   0   -35  6.25        $Upper R Arm
89      rcc  21.25 0   145   0   0   -35  6.25        $Upper L Arm
90      rcc -22.75 0   110   0   0   -35  4.85        $Lower R Arm
91      rcc  22.75 0   110   0   0   -35  4.85        $Lower L Arm
C
C Tank, surrounding concrete annulus
40      rcc  0   0 -1127.76   0   0 1127.76   1374.6   $ Outer cylinder
41      rcc  0   0 -1127.76   0   0 1015.84   1295.4   $ Inner cylinder
C Concrete (and port) Importance surfaces
60      pz   -13
61      pz   -27
62      pz   -40
69      pz   -54
70      pz   -67
71      pz   -80
72      pz   -93
C Sludge Importance surfaces
63      pz   -271
64      pz   -416
65      pz   -561
66      pz   -706
67      pz   -851
68      pz   -996
C Air Importance Surfaces
55      sph  450 0   90   100
56      sph  450 0   90   200
57      sph  450 0   90   300
58      sph  450 0   90   400
59      sph  450 0   90   500
C
C Outer Void
50      rcc  0   0  -15   0   0 400 1374.6       $ Coincide with tank radius

C =====Data=====
C
C
C *** PMMA *** (Lucite)
m208  1000           -0.080538      $PMMA
      6000           -0.599848
      8000           -0.319614
C
C Air, density=1.205e-3 g/cc
m101  7000           -0.755636      $N
      8000           -0.231475      $O
      18000          -0.012889      $Ar

```

ATTACHMENT B
DOSE MODELS
Page 3 of 35

C

C Ordinary Concrete, density = 2.3

m350	1000	-0.022100	\$H
	6000	-0.002484	\$C
	8000	-0.574930	\$O
	11000	-0.015208	\$Na
	12000	-0.001266	\$Mg
	13000	-0.019953	\$Al
	14000	-0.304627	\$Si
	19000	-0.010045	\$K
	20000	-0.042951	\$Ca
	26000	-0.006435	\$Fe

C

C Sludge, density = 1.23

m400	8000	0.363615281	\$O
	1000	0.139552217	\$H
	26000	0.009262229	\$Fe
	13000	0.015899426	\$Al
	25000	0.001868927	\$Mn
	20000	0.001329805	\$Ca
	6000	0.008161102	\$C
	9000	0.000331044	\$F
	7000	0.076349422	\$N
	19000	0.13292332	\$K
	16000	0.001907384	\$S
	24000	9.90221E-05	\$Cr
	47000	5.94086E-05	\$Ag
	12000	7.22305E-05	\$Mg
	29000	9.97572E-05	\$Cu
	58000	3.7862E-05	\$Ce
	15000	0.000181322	\$P
	56000	2.72846E-05	\$Ba
	57000	2.33286E-05	\$La
	80000	8.98041E-06	\$Hg
	27000	5.12576E-06	\$Co
	11000	0.247769977	\$Na
	14000	1.05915E-05	\$Si
	17000	0.000267783	\$Cl
	28000	6.14648E-07	\$Ni
	30000	8.03355E-05	\$Zn
	33000	4.89961E-06	\$As
	34000	2.8856E-05	\$Se
	38000	3.10603E-06	\$Sr
	40000	1.73449E-06	\$Zr
	48000	1.74539E-07	\$Cd
	55000	5.2383E-06	\$Cs
	60000	4.82667E-06	\$Nd
	82000	4.58187E-06	\$Pb

ATTACHMENT B
DOSE MODELS
Page 4 of 35

88226 2.80048E-06 \$Ra Note: radium requires isotope in zaid

C

C Translation for BOMAB Phantom

TR3 439 0 0 0 1 0 1 0 0 0 0 1 1 \$ Moved near port, rotated 90 degrees

C

mode p

imp:p

84934656 \$ Cell 120, BOMAB Phantom
84934656 \$ Cell 163, air - closest
56623104 \$ Cell 164, air
37748736 \$ Cell 165, air
25165824 \$ Cell 166, air
16777216 \$ Cell 167, air
16777216 \$ Cell 168, air - furthest
16777216 \$ Cell 169, concrete -closest
2097152 \$ Cell 170, concrete
262144 \$ Cell 171, concrete
32768 \$ Cell 172, concrete
4096 \$ Cell 181, concrete
512 \$ Cell 182, concrete
64 \$ Cell 183, concrete
8 \$ Cell 184, concrete - furthest
1 \$ Cell 174, sludge - closest
0 \$ Cell 199, void

sdef pos=450 0 0 erg=D10 rad=d20 axs=0 0 1 ext=d30

si20 0 700 \$ radius
sp20 -21 1 \$ even dist. radially
si30 L -1127 -127 \$ thickness
sp30 -21 0 \$ even dist. vertically
si10 sp10 \$ energy dist. in MeV
H D \$ energy bins then prob.
0 0
0.10 1.96E+01
0.20 1.47E+01
0.25 7.56E-02
0.30 5.88E-03
0.40 2.37E-02
0.60 5.19E+00
0.70 1.81E+01
0.80 6.57E+01
0.90 5.39E-01
1.00 2.79E-02
1.10 3.47E-01
1.20 1.66E-01
1.25 3.95E-02
1.30 7.41E-02
1.40 2.33E-01
1.60 4.28E-01

ATTACHMENT B
DOSE MODELS
Page 5 of 35

```
1.70      2.66E-04
1.80      5.47E-08
1.90      1.53E-06
2.00      2.56E-07
2.10      2.87E-05
2.20      1.03E+00
2.25      1.52E-08
2.30      2.00E-08
2.40      3.59E-08
2.60      1.61E-07
2.70      9.20E-44
2.80      8.71E-09
2.90      0.00E+00
3.00      6.88E-44
```

C

C Weigt windows based on IMP values

wwp:p 5 3 5 0 1

C

C Exponential Transform for sludge volume only

ext:p 0 14R 0.8 0

C Tallys

C

F5:p 450 0 140 20

C Energy Bins, more frequent at 0 - 0.1 MeV

C Bins specified by Taulbee

C

```
E5      0.010
        0.020
        0.030
        0.040
        0.050
        0.060
        0.070
        0.080
        0.090
        0.100
        0.110
        0.120
        0.130
        0.140
        0.150
        0.160
        0.170
        0.180
        0.190
        0.200
        0.210
        0.220
        0.230
```

ATTACHMENT B
DOSE MODELS
Page 6 of 35

0.240
0.250
0.300
0.350
0.400
0.450
0.500
1.000
1.500
2.000
2.500
3.000
3.500
4.000

FC5 *** Flux at 140 cm above surface *******

F15:p 450 0 90 20

C Energy Bins, more frequent at 0 - 0.1 MeV

C Bins specified by Taulbee

C

E15 0.010
0.020
0.030
0.040
0.050
0.060
0.070
0.080
0.090
0.100
0.110
0.120
0.130
0.140
0.150
0.160
0.170
0.180
0.190
0.200
0.210
0.220
0.230
0.240
0.250
0.300
0.350
0.400
0.450
0.500

ATTACHMENT B
DOSE MODELS
Page 7 of 35

1.000
1.500
2.000
2.500
3.000
3.500
4.000

FC15 *** Flux at 90 cm above surface *******

C ICRP 74 Table A.21 for H*(10) dose per fluence in pSv / cm²

#	DE0	DF0
0.01	0.0608	
0.015	0.8346	
0.02	1.0553	
0.03	0.8129	
0.04	0.64386	
0.05	0.54776	
0.06	0.50808	
0.08	0.52976	
0.1	0.6138	
0.15	0.894	
0.2	1.1984	
0.3	1.8078	
0.4	2.3814	
0.5	2.9274	
0.6	3.4364	
0.8	4.3911	
1	5.2299	
1.5	7.038	
2	8.5614	
3	11.1757	
4	13.44	
5	15.429	
6	17.538	
8	21.645	
10	25.52	

F25:p 450 0 90 20

C Energy Bins

E25 0.03 0.25 3.5

F35:p 450 0 40 20

C Energy Bins

E35 0.03 0.25 3.5

C ICRP 74 Table A.21 for H*(10) dose per fluence in pSv / cm²

#	DE25	DF25
0.01	0.0608	
0.015	0.8346	
0.02	1.0553	
0.03	0.8129	
0.04	0.64386	
0.05	0.54776	

ATTACHMENT B
DOSE MODELS
Page 8 of 35

0.06	0.50808
0.08	0.52976
0.1	0.6138
0.15	0.894
0.2	1.1984
0.3	1.8078
0.4	2.3814
0.5	2.9274
0.6	3.4364
0.8	4.3911
1	5.2299
1.5	7.038
2	8.5614
3	11.1757
4	13.44
5	15.429
6	17.538
8	21.645
10	25.52

#

DE35	DF35
0.01	0.0608
0.015	0.8346
0.02	1.0553
0.03	0.8129
0.04	0.64386
0.05	0.54776
0.06	0.50808
0.08	0.52976
0.1	0.6138
0.15	0.894
0.2	1.1984
0.3	1.8078
0.4	2.3814
0.5	2.9274
0.6	3.4364
0.8	4.3911
1	5.2299
1.5	7.038
2	8.5614
3	11.1757
4	13.44
5	15.429
6	17.538
8	21.645
10	25.52

nps 1E10

ATTACHMENT B
DOSE MODELS
Page 9 of 35

Dose Model for a Kneeling Worker – No Port

SRS **Dosimeter** Ratio Worker on top of Type III Tank

C

C Roger Halsey - March 2013

C

C Film Badge Model from Robert Morris

C BOMAB Model from Tim Taulbee

C

C =====Cells=====

C

C BOMAB Phantom

120 208 -1.19 -80:-81:-82:-83:-84:-85:-86:-87:-88:-89:-90:-91 TRCL=3

C

C Air

163	101	-0.001205	-55	40.2	#120
164	101	-0.001205	55	-56	40.2 #120
165	101	-0.001205	56	-57	-50 40.2
166	101	-0.001205	57	-58	-50 40.2
167	101	-0.001205	58	-59	-50 40.2
168	101	-0.001205	59	-50	40.2

C

C Concrete

169	350	-2.3	-40	60
170	350	-2.3	-40	-60 61
171	350	-2.3	-40	-61 62
172	350	-2.3	-40	-62 69
181	350	-2.3	-40	-69 70
182	350	-2.3	-40	-70 71
183	350	-2.3	-40	-71 72
184	350	-2.3	(-40 41 -72)	

C

C Sludge

174 400 -1.23 -41

C

C Void

199 0 (50 40.2) : (-40.2 40)

C =====Surfaces=====

C

C BOMAB Phantom, Kneeling

80	rcc	-7.5	-7.5	6	0	-40	0	6	\$Right Calf
81	rcc	7.5	-7.5	6	0	-40	0	6	\$Left Calf
82	rcc	-7.5	0	6	0	0	25	7.5	\$Right Thigh
83	rcc	7.5	0	6	0	0	25	7.5	\$Left Thigh
84	rec	0	0	31	0	0	20	18	0 0 0 10 0 \$Pelvis

ATTACHMENT B
DOSE MODELS
Page 10 of 35

85	rec	0	0	51	0	0	45	15	0	0	0	10	0	\$Chest
86	rcc	0	0	96	0	0	5	6.5						\$Neck
87	rec	0	0	101	0	0	20	7	0	0	0	9.5	0	\$Head
88	rcc	-21.25	0	96	0	0	-35	6.25						\$Upper R Arm
89	rcc	21.25	0	96	0	0	-35	6.25						\$Upper L Arm
90	rcc	-22.75	0	61	0	0	-35	4.85						\$Lower R Arm
91	rcc	22.75	0	61	0	0	-35	4.85						\$Lower L Arm

C

C Tank, surrounding concrete annulus

40	rcc	0	0	-1127.76	0	0	1127.76	1374.6	\$ Outer cylinder
41	rcc	0	0	-1127.76	0	0	1015.84	1295.4	\$ Inner cylinder

C Concrete (and port) Importance surfaces

60	pz	-13
61	pz	-27
62	pz	-40
69	pz	-54
70	pz	-67
71	pz	-80
72	pz	-93

C Sludge Importance surfaces

63	pz	-271
64	pz	-416
65	pz	-561
66	pz	-706
67	pz	-851
68	pz	-996

C Air Importance Surfaces

55	sph	450	0	90	100
56	sph	450	0	90	200
57	sph	450	0	90	300
58	sph	450	0	90	400
59	sph	450	0	90	500

C

C Outer Void

50	rcc	0	0	-15	0	0	400	1374.6	\$ Coincide with tank radius
----	------------	---	---	-----	---	---	-----	--------	------------------------------

C =====Data=====

C

C

C *** PMMA *** (Lucite)

m208	1000	-0.080538	\$PMMA
	6000	-0.599848	
	8000	-0.319614	

C

C Air, density=1.205e-3 g/cc

m101	7000	-0.755636	\$N
	8000	-0.231475	\$O

ATTACHMENT B
DOSE MODELS
Page 11 of 35

18000	-0.012889	\$Ar	
C			
C	Ordinary Concrete, density = 2.3		
m350	1000	-0.022100	\$H
	6000	-0.002484	\$C
	8000	-0.574930	\$O
	11000	-0.015208	\$Na
	12000	-0.001266	\$Mg
	13000	-0.019953	\$Al
	14000	-0.304627	\$Si
	19000	-0.010045	\$K
	20000	-0.042951	\$Ca
	26000	-0.006435	\$Fe
C			
C	Sludge, density = 1.23		
m400	8000	0.363615281	\$O
	1000	0.139552217	\$H
	26000	0.009262229	\$Fe
	13000	0.015899426	\$Al
	25000	0.001868927	\$Mn
	20000	0.001329805	\$Ca
	6000	0.008161102	\$C
	9000	0.000331044	\$F
	7000	0.076349422	\$N
	19000	0.13292332	\$K
	16000	0.001907384	\$S
	24000	9.90221E-05	\$Cr
	47000	5.94086E-05	\$Ag
	12000	7.22305E-05	\$Mg
	29000	9.97572E-05	\$Cu
	58000	3.7862E-05	\$Ce
	15000	0.000181322	\$P
	56000	2.72846E-05	\$Ba
	57000	2.33286E-05	\$La
	80000	8.98041E-06	\$Hg
	27000	5.12576E-06	\$Co
	11000	0.247769977	\$Na
	14000	1.05915E-05	\$Si
	17000	0.000267783	\$Cl
	28000	6.14648E-07	\$Ni
	30000	8.03355E-05	\$Zn
	33000	4.89961E-06	\$As
	34000	2.8856E-05	\$Se
	38000	3.10603E-06	\$Sr
	40000	1.73449E-06	\$Zr
	48000	1.74539E-07	\$Cd
	55000	5.2383E-06	\$Cs
	60000	4.82667E-06	\$Nd

ATTACHMENT B
DOSE MODELS
Page 12 of 35

```
82000  4.58187E-06      $Pb
88226  2.80048E-06      $Ra Note: radium requires isotope in zaid
C
C Translation for BOMAB Phantom
TR3 439 0 0 0 1 0 1 0 0 0 0 1 1   $ Moved near port, rotated 90 degrees
C
mode p
imp:p
 84934656      $ Cell 120, BOMAB Phantom
 84934656      $ Cell 163, air - closest
 56623104      $ Cell 164, air
 37748736      $ Cell 165, air
 25165824      $ Cell 166, air
 16777216      $ Cell 167, air
 16777216      $ Cell 168, air - furthest
 16777216      $ Cell 169, concrete -closest
 2097152       $ Cell 170, concrete
 262144        $ Cell 171, concrete
 32768         $ Cell 172, concrete
 4096          $ Cell 181, concrete
 512           $ Cell 182, concrete
 64            $ Cell 183, concrete
 8             $ Cell 184, concrete - furthest
 1             $ Cell 174, sludge - closest
 0             $ Cell 199, void
sdef pos=450 0 0 erg=D10 rad=d20 axs=0 0 1 ext=d30
si20 0 700          $ radius
sp20 -21 1          $ even dist. radially
si30 L -1127 -127  $ thickness
sp30 -21 0          $ even dist. vertically
#    si10  sp10      $ energy dist. in MeV
      H    D          $ energy bins then prob.
      0    0
      0.10 1.96E+01
      0.20 1.47E+01
      0.25 7.56E-02
      0.30 5.88E-03
      0.40 2.37E-02
      0.60 5.19E+00
      0.70 1.81E+01
      0.80 6.57E+01
      0.90 5.39E-01
      1.00 2.79E-02
      1.10 3.47E-01
      1.20 1.66E-01
      1.25 3.95E-02
      1.30 7.41E-02
      1.40 2.33E-01
```

ATTACHMENT B
DOSE MODELS
Page 13 of 35

```
1.60      4.28E-01
1.70      2.66E-04
1.80      5.47E-08
1.90      1.53E-06
2.00      2.56E-07
2.10      2.87E-05
2.20      1.03E+00
2.25      1.52E-08
2.30      2.00E-08
2.40      3.59E-08
2.60      1.61E-07
2.70      9.20E-44
2.80      8.71E-09
2.90      0.00E+00
3.00      6.88E-44
```

C

C Weigt windows based on IMP values

wwp:p 5 3 5 0 1

C

C Exponential Transform for sludge volume only

ext:p 0 14R 0.8 0

C Tallys

C

FC5 *** Flux at 90 cm above surface *******

F5:p 450 0 90 10

C Energy Bins, more frequent at 0 - 0.1 MeV

C Bins specified by Taulbee

C

```
E5      0.010
        0.020
        0.030
        0.040
        0.050
        0.060
        0.070
        0.080
        0.090
        0.100
        0.110
        0.120
        0.130
        0.140
        0.150
        0.160
        0.170
        0.180
        0.190
        0.200
        0.210
```

ATTACHMENT B
DOSE MODELS
Page 14 of 35

0.220
0.230
0.240
0.250
0.300
0.350
0.400
0.450
0.500
0.600
0.700
0.800
0.900
1.000
1.100
1.200
1.300
1.400
1.500
1.600
1.700
1.800
1.900
2.000
2.100
2.200
2.300
2.400
2.500
2.600
2.700
2.800
2.900
3.000

FC15 *** Flux at 40 cm above surface *******

F15:p 450 0 40 10

C Energy Bins, more frequent at 0 - 0.1 MeV

C Bins specified by Taulbee

C

E15 0.010
 0.020
 0.030
 0.040
 0.050
 0.060
 0.070
 0.080
 0.090
 0.100

ATTACHMENT B
DOSE MODELS
Page 15 of 35

0.110
0.120
0.130
0.140
0.150
0.160
0.170
0.180
0.190
0.200
0.210
0.220
0.230
0.240
0.250
0.300
0.350
0.400
0.450
0.500
0.600
0.700
0.800
0.900
1.000
1.100
1.200
1.300
1.400
1.500
1.600
1.700
1.800
1.900
2.000
2.100
2.200
2.300
2.400
2.500
2.600
2.700
2.800
2.900
3.000

FC25 ***** ICRP 74 Dose at 90 cm above surface *****

F25:p 450 0 90 10

C Energy Bins

E25 0.03 0.25 3.5

ATTACHMENT B
DOSE MODELS
Page 16 of 35

C ICRP 74 Table A.21 for H*(10) dose per fluence in pSv / cm²

#	DE25	DF25
0.01	0.0608	
0.015	0.8346	
0.02	1.0553	
0.03	0.8129	
0.04	0.64386	
0.05	0.54776	
0.06	0.50808	
0.08	0.52976	
0.1	0.6138	
0.15	0.894	
0.2	1.1984	
0.3	1.8078	
0.4	2.3814	
0.5	2.9274	
0.6	3.4364	
0.8	4.3911	
1	5.2299	
1.5	7.038	
2	8.5614	
3	11.1757	
4	13.44	
5	15.429	
6	17.538	
8	21.645	
10	25.52	

FC35 *** ICRP 74 Dose at 40 cm above surface *******

F35:p 450 0 40 10

C Energy Bins

E35 0.03 0.25 3.5

C ICRP 74 Table A.21 for H*(10) dose per fluence in pSv / cm²

#	DE35	DF35
0.01	0.0608	
0.015	0.8346	
0.02	1.0553	
0.03	0.8129	
0.04	0.64386	
0.05	0.54776	
0.06	0.50808	
0.08	0.52976	
0.1	0.6138	
0.15	0.894	
0.2	1.1984	
0.3	1.8078	
0.4	2.3814	
0.5	2.9274	
0.6	3.4364	
0.8	4.3911	

ATTACHMENT B
DOSE MODELS
Page 17 of 35

1	5.2299
1.5	7.038
2	8.5614
3	11.1757
4	13.44
5	15.429
6	17.538
8	21.645
10	25.52

nps 1E10

rand seed = 7777777777777777

ATTACHMENT B
DOSE MODELS
Page 18 of 35

Dose Model for a Standing Worker Near a Port

SRS **Dosimeter** Ratio Worker on top of Type III Tank

C

C Roger Halsey - March 2013

C

C Film Badge Model from Robert Morris

C BOMAB Model from Tim Taulbee

C

C =====Cells=====

C

C BOMAB Phantom

120 208 -1.19 -80:-81:-82:-83:-84:-85:-86:-87:-88:-89:-90:-91 TRCL=3

C

C Air

163	101	-0.001205	-55	40.2	#120	
164	101	-0.001205	55	-56	40.2	#120
165	101	-0.001205	56	-57	-50	40.2
166	101	-0.001205	57	-58	-50	40.2
167	101	-0.001205	58	-59	-50	40.2
168	101	-0.001205	59	-50	40.2	

C Port

103	101	-0.001205	-40.2	60	-43
104	101	-0.001205	-60	61	-43
105	101	-0.001205	-61	62	-43
106	101	-0.001205	-62	69	-43
107	101	-0.001205	-69	70	-43
108	101	-0.001205	-70	71	-43
109	101	-0.001205	-71	72	-43
110	101	-0.001205	-72	41.2	-43

C

C Concrete

169	350	-2.3	-40	43	60	
170	350	-2.3	-40	43	-60	61
171	350	-2.3	-40	43	-61	62
172	350	-2.3	-40	43	-62	69
181	350	-2.3	-40	43	-69	70
182	350	-2.3	-40	43	-70	71
183	350	-2.3	-40	43	-71	72
184	350	-2.3	(-40	41	43	-72)

C

C Sludge

174 400 -1.23 -41

C

C Void

199 0 (50 40.2) : (-40.2 40)

C =====Surfaces=====

ATTACHMENT B
DOSE MODELS
Page 19 of 35

=

C

C BOMAB Phantom, Standing

80	rcc	-7.5	0	0	0	40	6		\$Right Calf	
81	rcc	7.5	0	0	0	40	6		\$Left Calf	
82	rcc	-7.5	0	40	0	0	40	7.5	\$Right Thigh	
83	rcc	7.5	0	40	0	0	40	7.5	\$Left Thigh	
84	rec	0	0	80	0	0	20	18	0 0 0 10 0	\$Pelvis
85	rec	0	0	100	0	0	45	15	0 0 0 10 0	\$Chest
86	rcc	0	0	145	0	0	5	6.5		\$Neck
87	rec	0	0	150	0	0	20	7	0 0 0 9.5 0	\$Head
88	rcc	-21.25	0	145	0	0	-35	6.25		\$Upper R Arm
89	rcc	21.25	0	145	0	0	-35	6.25		\$Upper L Arm
90	rcc	-22.75	0	110	0	0	-35	4.85		\$Lower R Arm
91	rcc	22.75	0	110	0	0	-35	4.85		\$Lower L Arm

C

C Tank, surrounding concrete annulus

40	rcc	0	0	-1127.76	0	0	1127.76	1374.6	\$ Outer cylinder
41	rcc	0	0	-1127.76	0	0	1015.84	1295.4	\$ Inner cylinder
43	c/z	500	0	15					\$ air sample port

C Concrete (and port) Importance surfaces

60	pz	-13
61	pz	-27
62	pz	-40
69	pz	-54
70	pz	-67
71	pz	-80
72	pz	-93

C Sludge Importance surfaces

63	pz	-271
64	pz	-416
65	pz	-561
66	pz	-706
67	pz	-851
68	pz	-996

C Air Importance Surfaces

55	sph	450	0	90	100
56	sph	450	0	90	200
57	sph	450	0	90	300
58	sph	450	0	90	400
59	sph	450	0	90	500

C

C Outer Void

50	rcc	0	0	-15	0	0	400	1374.6	\$ Coincide with tank radius
----	------------	---	---	-----	---	---	-----	--------	------------------------------

C =====Data=====

C

ATTACHMENT B
DOSE MODELS
Page 20 of 35

C
C *** PMMA *** (Lucite)
m208 1000 -0.080538 \$PMMA
6000 -0.599848
8000 -0.319614

C
C Air, density=1.205e-3 g/cc
m101 7000 -0.755636 \$N
8000 -0.231475 \$O
18000 -0.012889 \$Ar

C
C Ordinary Concrete, density = 2.3
m350 1000 -0.022100 \$H
6000 -0.002484 \$C
8000 -0.574930 \$O
11000 -0.015208 \$Na
12000 -0.001266 \$Mg
13000 -0.019953 \$Al
14000 -0.304627 \$Si
19000 -0.010045 \$K
20000 -0.042951 \$Ca
26000 -0.006435 \$Fe

C
C Sludge, density = 1.23
m400
8000 0.363615281 \$O
1000 0.139552217 \$H
26000 0.009262229 \$Fe
13000 0.015899426 \$Al
25000 0.001868927 \$Mn
20000 0.001329805 \$Ca
6000 0.008161102 \$C
9000 0.000331044 \$F
7000 0.076349422 \$N
19000 0.13292332 \$K
16000 0.001907384 \$S
24000 9.90221E-05 \$Cr
47000 5.94086E-05 \$Ag
12000 7.22305E-05 \$Mg
29000 9.97572E-05 \$Cu
58000 3.7862E-05 \$Ce
15000 0.000181322 \$P
56000 2.72846E-05 \$Ba
57000 2.33286E-05 \$La
80000 8.98041E-06 \$Hg
27000 5.12576E-06 \$Co
11000 0.247769977 \$Na
14000 1.05915E-05 \$Si
17000 0.000267783 \$Cl

ATTACHMENT B
DOSE MODELS
Page 21 of 35

```

28000  6.14648E-07    $Ni
30000  8.03355E-05    $Zn
33000  4.89961E-06    $As
34000  2.8856E-05     $Se
38000  3.10603E-06    $Sr
40000  1.73449E-06    $Zr
48000  1.74539E-07    $Cd
55000  5.2383E-06     $Cs
60000  4.82667E-06    $Nd
82000  4.58187E-06    $Pb
88226  2.80048E-06    $Ra Note: radium requires isotope in zaid

```

C

C Translation for BOMAB Phantom

TR3 439 0 0 0 1 0 1 0 0 0 0 1 1 \$ Moved near port, rotated 90 degrees

C

mode p**imp:p**

```

84934656      $ Cell 120, BOMAB Phantom
84934656      $ Cell 163, air - closest
56623104      $ Cell 164, air
37748736      $ Cell 165, air
25165824      $ Cell 166, air
16777216      $ Cell 167, air
16777216      $ Cell 168, air - furthest
16777216      $ Cell 103, Port- closest
2097152       $ Cell 104, Port
262144        $ Cell 105, Port
32768         $ Cell 106, Port
4096          $ Cell 107, Port
512           $ Cell 108, Port
64             $ Cell 109, Port
8              $ Cell 110, Port - furthest
16777216      $ Cell 169, concrete -closest
2097152       $ Cell 170, concrete
262144        $ Cell 171, concrete
32768         $ Cell 172, concrete
4096          $ Cell 181, concrete
512           $ Cell 182, concrete
64             $ Cell 183, concrete
8              $ Cell 184, concrete - furthest
1              $ Cell 174, sludge - closest
0              $ Cell 199, void

```

sdef pos=450 0 0 erg=D10 rad=d20 axs=0 0 1 ext=d30

```

si20  0 700          $ radius
sp20  -21 1          $ even dist. radially
si30  L -1127 -127   $ thickness
sp30  -21 0          $ even dist. vertically
#     si10  sp10       $ energy dist. in MeV

```

ATTACHMENT B
DOSE MODELS
Page 22 of 35

H	D	\$ energy bins then prob.
0	0	
0.10	5.51E-04	
0.20	9.82E-04	
0.25	2.91E-04	
0.30	2.03E-04	
0.40	2.62E-04	
0.60	3.35E-04	
0.70	1.24E-04	
0.80	1.13E-04	
0.90	1.05E-04	
1.00	9.91E-05	
1.10	9.29E-05	
1.20	8.94E-05	
1.25	4.23E-05	
1.30	3.97E-05	
1.40	7.56E-05	
1.60	1.40E-04	
1.70	6.19E-05	
1.80	5.61E-05	
1.90	5.22E-05	
2.00	4.63E-05	
2.10	3.80E-05	
2.20	3.24E-05	
2.25	1.31E-05	
2.30	1.29E-05	
2.40	2.04E-05	
2.60	2.81E-05	
2.70	6.96E-06	
2.80	4.70E-06	
2.90	2.57E-06	
3.00	1.64E-06	
3.10	1.23E-06	
3.20	1.10E-06	
3.25	2.89E-07	
3.30	1.68E-07	
3.40	4.92E-07	
3.60	5.80E-08	

C

C DXRAN Spheres at entrance and exit of port

DXT:p 500 0 0 15 15 500 0 -111.92 15 15 450 0 115 100 100

C

C Weigt windows based on IMP values

wwp:p 5 3 5 0 1

C

C Exponential Transform for sludge volume only

ext:p 0 22R 0.8 0

C Tallys

C

ATTACHMENT B
DOSE MODELS
Page 23 of 35

F5:p 450 0 140 20
C Energy Bins, more frequent at 0 - 0.1 MeV
C Bins specified by Taulbee

C
E5 0.010
 0.020
 0.030
 0.040
 0.050
 0.060
 0.070
 0.080
 0.090
 0.100
 0.110
 0.120
 0.130
 0.140
 0.150
 0.160
 0.170
 0.180
 0.190
 0.200
 0.210
 0.220
 0.230
 0.240
 0.250
 0.300
 0.350
 0.400
 0.450
 0.500
 1.000
 1.500
 2.000
 2.500
 3.000
 3.500
 4.000

FC5 *** Flux at 140 cm above surface *******

F15:p 450 0 90 20
C Energy Bins, more frequent at 0 - 0.1 MeV
C Bins specified by Taulbee

C
E15 0.010
 0.020
 0.030

ATTACHMENT B
DOSE MODELS
Page 24 of 35

0.040
0.050
0.060
0.070
0.080
0.090
0.100
0.110
0.120
0.130
0.140
0.150
0.160
0.170
0.180
0.190
0.200
0.210
0.220
0.230
0.240
0.250
0.300
0.350
0.400
0.450
0.500
1.000
1.500
2.000
2.500
3.000
3.500
4.000

FC15 *** Flux at 90 cm above surface *******

C ICRP 74 Table A.21 for H*(10) dose per fluence in pSv / cm²

#	DE0	DF0
	0.01	0.0608
	0.015	0.8346
	0.02	1.0553
	0.03	0.8129
	0.04	0.64386
	0.05	0.54776
	0.06	0.50808
	0.08	0.52976
	0.1	0.6138
	0.15	0.894
	0.2	1.1984
	0.3	1.8078

ATTACHMENT B
DOSE MODELS
Page 25 of 35

0.4 2.3814
0.5 2.9274
0.6 3.4364
0.8 4.3911
1 5.2299
1.5 7.038
2 8.5614
3 11.1757
4 13.44
5 15.429
6 17.538
8 21.645
10 25.52

F25:p 450 0 90 20

C Energy Bins

E25 0.03 0.25 3.5

F35:p 450 0 40 20

C Energy Bins

E35 0.03 0.25 3.5

C ICRP 74 Table A.21 for H*(10) dose per fluence in pSv / cm²

#	DE25	DF25
	0.01	0.0608
	0.015	0.8346
	0.02	1.0553
	0.03	0.8129
	0.04	0.64386
	0.05	0.54776
	0.06	0.50808
	0.08	0.52976
	0.1	0.6138
	0.15	0.894
	0.2	1.1984
	0.3	1.8078
	0.4	2.3814
	0.5	2.9274
	0.6	3.4364
	0.8	4.3911
	1	5.2299
	1.5	7.038
	2	8.5614
	3	11.1757
	4	13.44
	5	15.429
	6	17.538
	8	21.645
	10	25.52
#	DE35	DF35
	0.01	0.0608
	0.015	0.8346

ATTACHMENT B
DOSE MODELS
Page 26 of 35

0.02	1.0553
0.03	0.8129
0.04	0.64386
0.05	0.54776
0.06	0.50808
0.08	0.52976
0.1	0.6138
0.15	0.894
0.2	1.1984
0.3	1.8078
0.4	2.3814
0.5	2.9274
0.6	3.4364
0.8	4.3911
1	5.2299
1.5	7.038
2	8.5614
3	11.1757
4	13.44
5	15.429
6	17.538
8	21.645
10	25.52

nps 1E10

ATTACHMENT B
DOSE MODELS
Page 27 of 35

Dose Model for a Kneeling Worker Near a Port

SRS **Dosimeter** Ratio Worker on top of Type III Tank

C

C Roger Halsey - March 2013

C

C Film Badge Model from Robert Morris

C BOMAB Model from Tim Taulbee

C

C =====Cells=====

C

C BOMAB Phantom

120 208 -1.19 -80:-81:-82:-83:-84:-85:-86:-87:-88:-89:-90:-91 TRCL=3

C

C Air

163	101	-0.001205	-55	40.2	#120	
164	101	-0.001205	55	-56	40.2	#120
165	101	-0.001205	56	-57	-50	40.2
166	101	-0.001205	57	-58	-50	40.2
167	101	-0.001205	58	-59	-50	40.2
168	101	-0.001205	59	-50	40.2	

C Port

103	101	-0.001205	-40.2	60	-43
104	101	-0.001205	-60	61	-43
105	101	-0.001205	-61	62	-43
106	101	-0.001205	-62	69	-43
107	101	-0.001205	-69	70	-43
108	101	-0.001205	-70	71	-43
109	101	-0.001205	-71	72	-43
110	101	-0.001205	-72	41.2	-43

C

C Concrete

169	350	-2.3	-40	43	60	
170	350	-2.3	-40	43	-60	61
171	350	-2.3	-40	43	-61	62
172	350	-2.3	-40	43	-62	69
181	350	-2.3	-40	43	-69	70
182	350	-2.3	-40	43	-70	71
183	350	-2.3	-40	43	-71	72
184	350	-2.3	(-40	41	43	-72)

C

C Sludge

174 400 -1.23 -41

C

C Void

199 0 (50 40.2) : (-40.2 40)

C =====Surfaces=====

ATTACHMENT B**DOSE MODELS**

Page 28 of 35

=

C

C BOMAB Phantom, Kneeling

80	rcc	-7.5	-7.5	6	0	-40	0	6		\$Right Calf
81	rcc	7.5	-7.5	6	0	-40	0	6		\$Left Calf
82	rcc	-7.5	0	6	0	0	25	7.5		\$Right Thigh
83	rcc	7.5	0	6	0	0	25	7.5		\$Left Thigh
84	rec	0	0	31	0	0	20	18	0	\$Pelvis
85	rec	0	0	51	0	0	45	15	0	\$Chest
86	rcc	0	0	96	0	0	5	6.5		\$Neck
87	rec	0	0	101	0	0	20	7	0	\$Head
88	rcc	-21.25	0	96	0	0	-35	6.25		\$Upper R Arm
89	rcc	21.25	0	96	0	0	-35	6.25		\$Upper L Arm
90	rcc	-22.75	0	61	0	0	-35	4.85		\$Lower R Arm
91	rcc	22.75	0	61	0	0	-35	4.85		\$Lower L Arm

C

C Tank, surrounding concrete annulus

40	rcc	0	0	-1127.76	0	0	1127.76	1374.6	\$ Outer cylinder
41	rcc	0	0	-1127.76	0	0	1015.84	1295.4	\$ Inner cylinder
43	c/z	500	0	15					\$ air sample port

C Concrete (and port) Importance surfaces

60	pz	-13
61	pz	-27
62	pz	-40
69	pz	-54
70	pz	-67
71	pz	-80
72	pz	-93

C Sludge Importance surfaces

63	pz	-271
64	pz	-416
65	pz	-561
66	pz	-706
67	pz	-851
68	pz	-996

C Air Importance Surfaces

55	sph	450	0	90	100
56	sph	450	0	90	200
57	sph	450	0	90	300
58	sph	450	0	90	400
59	sph	450	0	90	500

C

C Outer Void

50	rcc	0	0	-15	0	0	400	1374.6	\$ Coincide with tank radius
----	------------	---	---	-----	---	---	-----	--------	------------------------------

C =====Data=====

C

ATTACHMENT B
DOSE MODELS
Page 29 of 35

C
C *** PMMA *** (Lucite)
m208 1000 -0.080538 \$PMMA
6000 -0.599848
8000 -0.319614

C
C Air, density=1.205e-3 g/cc
m101 7000 -0.755636 \$N
8000 -0.231475 \$O
18000 -0.012889 \$Ar

C
C Ordinary Concrete, density = 2.3
m350 1000 -0.022100 \$H
6000 -0.002484 \$C
8000 -0.574930 \$O
11000 -0.015208 \$Na
12000 -0.001266 \$Mg
13000 -0.019953 \$Al
14000 -0.304627 \$Si
19000 -0.010045 \$K
20000 -0.042951 \$Ca
26000 -0.006435 \$Fe

C
C Sludge, density = 1.23
m400
8000 0.363615281 \$O
1000 0.139552217 \$H
26000 0.009262229 \$Fe
13000 0.015899426 \$Al
25000 0.001868927 \$Mn
20000 0.001329805 \$Ca
6000 0.008161102 \$C
9000 0.000331044 \$F
7000 0.076349422 \$N
19000 0.13292332 \$K
16000 0.001907384 \$S
24000 9.90221E-05 \$Cr
47000 5.94086E-05 \$Ag
12000 7.22305E-05 \$Mg
29000 9.97572E-05 \$Cu
58000 3.7862E-05 \$Ce
15000 0.000181322 \$P
56000 2.72846E-05 \$Ba
57000 2.33286E-05 \$La
80000 8.98041E-06 \$Hg
27000 5.12576E-06 \$Co
11000 0.247769977 \$Na
14000 1.05915E-05 \$Si
17000 0.000267783 \$Cl

ATTACHMENT B
DOSE MODELS
Page 30 of 35

28000	6.14648E-07	\$Ni
30000	8.03355E-05	\$Zn
33000	4.89961E-06	\$As
34000	2.8856E-05	\$Se
38000	3.10603E-06	\$Sr
40000	1.73449E-06	\$Zr
48000	1.74539E-07	\$Cd
55000	5.2383E-06	\$Cs
60000	4.82667E-06	\$Nd
82000	4.58187E-06	\$Pb
88226	2.80048E-06	\$Ra Note: radium requires isotope in zaid

C

C Translation for BOMAB Phantom

TR3 439 0 0 0 1 0 1 0 0 0 0 1 1 \$ Moved near port, rotated 90 degrees

C

mode p**imp:p**

84934656	\$ Cell 120, BOMAB Phantom
84934656	\$ Cell 163, air - closest
56623104	\$ Cell 164, air
37748736	\$ Cell 165, air
25165824	\$ Cell 166, air
16777216	\$ Cell 167, air
16777216	\$ Cell 168, air - furthest
16777216	\$ Cell 103, Port- closest
2097152	\$ Cell 104, Port
262144	\$ Cell 105, Port
32768	\$ Cell 106, Port
4096	\$ Cell 107, Port
512	\$ Cell 108, Port
64	\$ Cell 109, Port
8	\$ Cell 110, Port - furthest
16777216	\$ Cell 169, concrete -closest
2097152	\$ Cell 170, concrete
262144	\$ Cell 171, concrete
32768	\$ Cell 172, concrete
4096	\$ Cell 181, concrete
512	\$ Cell 182, concrete
64	\$ Cell 183, concrete
8	\$ Cell 184, concrete - furthest
1	\$ Cell 174, sludge - closest
0	\$ Cell 199, void

sdef pos=450 0 0 erg=D10 rad=d20 axs=0 0 1 ext=d30**si20** 0 700 \$ radius**sp20** -21 1 \$ even dist. radially**si30** L -1127 -127 \$ thickness**sp30** -21 0 \$ even dist. vertically# **si10** **sp10** \$ energy dist. in MeV

ATTACHMENT B
DOSE MODELS
Page 31 of 35

H	D	\$ energy bins then prob.
0	0	
0.10	1.96E+01	
0.20	1.47E+01	
0.25	7.56E-02	
0.30	5.88E-03	
0.40	2.37E-02	
0.60	5.19E+00	
0.70	1.81E+01	
0.80	6.57E+01	
0.90	5.39E-01	
1.00	2.79E-02	
1.10	3.47E-01	
1.20	1.66E-01	
1.25	3.95E-02	
1.30	7.41E-02	
1.40	2.33E-01	
1.60	4.28E-01	
1.70	2.66E-04	
1.80	5.47E-08	
1.90	1.53E-06	
2.00	2.56E-07	
2.10	2.87E-05	
2.20	1.03E+00	
2.25	1.52E-08	
2.30	2.00E-08	
2.40	3.59E-08	
2.60	1.61E-07	
2.70	9.20E-44	
2.80	8.71E-09	
2.90	0.00E+00	
3.00	6.88E-44	

C

C DXRAN Spheres at entrance and exit of port

DXT:p 500 0 0 15 15 500 0 -111.92 15 15 450 0 115 100 100

C

C Weigt windows based on IMP values

wwp:p 5 3 5 0 1

C

C Exponential Transform for sludge volume only

ext:p 0 22R 0.8 0

C Tallys

C

F5:p 450 0 140 20

C Energy Bins, more frequent at 0 - 0.1 MeV

C Bins specified by Taulbee

C

E5 0.010
0.020

ATTACHMENT B
DOSE MODELS
Page 32 of 35

0.030
0.040
0.050
0.060
0.070
0.080
0.090
0.100
0.110
0.120
0.130
0.140
0.150
0.160
0.170
0.180
0.190
0.200
0.210
0.220
0.230
0.240
0.250
0.300
0.350
0.400
0.450
0.500
1.000
1.500
2.000
2.500
3.000
3.500
4.000

FC5 *** Flux at 140 cm above surface *******

F15:p 450 0 90 20

C Energy Bins, more frequent at 0 - 0.1 MeV

C Bins specified by Taulbee

C

E15 0.010
0.020
0.030
0.040
0.050
0.060
0.070
0.080
0.090

ATTACHMENT B
DOSE MODELS
Page 33 of 35

0.100
0.110
0.120
0.130
0.140
0.150
0.160
0.170
0.180
0.190
0.200
0.210
0.220
0.230
0.240
0.250
0.300
0.350
0.400
0.450
0.500
1.000
1.500
2.000
2.500
3.000
3.500
4.000

FC15 *** Flux at 90 cm above surface *******

C ICRP 74 Table A.21 for $H^*(10)$ dose per fluence in pSv / cm²

#	DE0	DF0
0.01	0.0608	
0.015	0.8346	
0.02	1.0553	
0.03	0.8129	
0.04	0.64386	
0.05	0.54776	
0.06	0.50808	
0.08	0.52976	
0.1	0.6138	
0.15	0.894	
0.2	1.1984	
0.3	1.8078	
0.4	2.3814	
0.5	2.9274	
0.6	3.4364	
0.8	4.3911	
1	5.2299	
1.5	7.038	

ATTACHMENT B
DOSE MODELS
Page 34 of 35

2 8.5614
3 11.1757
4 13.44
5 15.429
6 17.538
8 21.645
10 25.52
F25:p 450 0 90 20
C Energy Bins
E25 0.03 0.25 3.5
F35:p 450 0 40 20
C Energy Bins
E35 0.03 0.25 3.5
C ICRP 74 Table A.21 for H*(10) dose per fluence in pSv / cm²
DE25 **DF25**
0.01 0.0608
0.015 0.8346
0.02 1.0553
0.03 0.8129
0.04 0.64386
0.05 0.54776
0.06 0.50808
0.08 0.52976
0.1 0.6138
0.15 0.894
0.2 1.1984
0.3 1.8078
0.4 2.3814
0.5 2.9274
0.6 3.4364
0.8 4.3911
1 5.2299
1.5 7.038
2 8.5614
3 11.1757
4 13.44
5 15.429
6 17.538
8 21.645
10 25.52
DE35 **DF35**
0.01 0.0608
0.015 0.8346
0.02 1.0553
0.03 0.8129
0.04 0.64386
0.05 0.54776
0.06 0.50808
0.08 0.52976

ATTACHMENT B
DOSE MODELS
Page 35 of 35

0 . 1	0 . 6138
0 . 15	0 . 894
0 . 2	1 . 1984
0 . 3	1 . 8078
0 . 4	2 . 3814
0 . 5	2 . 9274
0 . 6	3 . 4364
0 . 8	4 . 3911
1	5 . 2299
1 . 5	7 . 038
2	8 . 5614
3	11 . 1757
4	13 . 44
5	15 . 429
6	17 . 538
8	21 . 645
10	25 . 52

nps 1E10

ATTACHMENT C
FILM BADGE MODEL
Page 1 of 6

This model was repeated for each measurement point using the values listed in Attachment A as the source spectrum.

MCNPX Visual Editor Version X_24E
C Created on: Monday, May 20, 2013 at 14:25
C Savannah River Dosimeter Badge PHOTON VERSION
C
C
C *** Film *** (7 Cell)
21 2 -1.4 21 -22 23 -24 46 -49 \$ Film (Pb region)
22 2 -1.4 21 -22 23 -25 45 -46 \$ Film (Ag)
23 2 -1.4 21 -22 25 -24 45 -46 \$ Film (Air)
24 2 -1.4 21 -22 23 -25 44 -45 \$ Film (Al)
25 2 -1.4 21 -22 25 -24 44 -45 \$ Film (Nylon)
28 9 -1.39 31 -21 23 -24 44 -49 \$ Front Mylar
29 9 -1.39 22 -32 23 -24 44 -49 \$ Back Mylar
C
C *** Front Filter Set (9 cells)
31 252 -11.35 33 -31 23 -24 46 -49 \$ Front Filter (Pb)
32 7 -10.5 33 -31 23 -25 45 -46 \$ Front Filter (Ag)
33 204 -0.001205 33 -31 25 -24 45 -46 \$ Front Open Filter (Air)
34 208 -2.6989 33 -31 23 -25 44 -45 \$ Front Filter (Al)
35 4 -1.14 33 -31 25 -24 44 -45 \$ Front Filter (Nylon)
36 204 -0.001205 35 -33 23 -24 \$ Air Volume Above Additional Al thickness
 45 -49
37 204 -0.001205 35 -33 25 -24 \$ Air Volume Beside additional Al thickness
 44 -45
38 208 -2.6989 35 -33 23 -25 44 -45 \$ Additional 1 mm Al thickness
39 3 -1.42 37 -35 23 -24 44 -49 \$ Plastic Identification Cover
C
C *** Back Filter Set (9 cells)
41 252 -11.35 32 -34 23 -24 46 -49 \$ Front Filter (Pb)
42 7 -10.5 32 -34 23 -25 45 -46 \$ Front Filter (Ag)
43 204 -0.001205 32 -34 25 -24 45 -46 \$ Front Open Filter (Air)
44 208 -2.6989 32 -34 23 -25 44 -45 \$ Front Filter (Al)
45 4 -1.14 32 -34 25 -24 44 -45 \$ Front Filter (Nylon)
46 204 -0.001205 34 -36 23 -24 \$ Air Volume Above Additional Al thickness
 45 -49
47 204 -0.001205 34 -36 25 -24 \$ Air Volume Beside additional Al thicknes
 44 -45
48 208 -2.6989 34 -36 23 -25 44 -45 \$ Additional 1 mm Al thickness
49 3 -1.42 36 -38 23 -24 44 -49 \$ Plastic Identification Cover
C
C *** Dosimeter Cover (Plastic) (4 Cells)
52 4 -1.14 37 -38 23 -24 51 -44 \$ Dosimeter Bottom
53 4 -1.14 37 -38 23 -24 49 -52 \$ Dosimeter Top
54 4 -1.14 37 -38 24 -27 51 -52 \$ Dosimeter Right Side
55 4 -1.14 37 -38 26 -23 51 -52 \$ Dosimeter Left Side
C
C *** Modifier Cells (2 Cells)
61 8 -1.19 -61 \$ PMMA Phantom
C
C *** Outer Boundaries *** (2 Cells)

ATTACHMENT C
FILM BADGE MODEL
Page 2 of 6

98 204 -0.001205 (-37 :38 :-26 :27 :-51 :52)61 -89 \$ Air Volume
99 0 89 \$ Outside Universe

C ***** Surface Cards

C *** Film Thickness

21 px -0.0019
22 px 0.0019

C

C *** Savannah Dosimeter y-axis planes

23 py -1.5 \$ Film left boundary
24 py 1.5 \$ Film right boundary
25 py 0 \$ Film centerline
26 py -1.75 \$ Dosimeter left boundary
27 py 1.75 \$ Dosimeter right boundary

C

C *** Savannah Dosimeter x-axis Layers

31 px -0.0034 \$ Front Mylar
32 px 0.0034 \$ Back Mylar
33 px -0.1034 \$ Front Filter (1 mm)
34 px 0.1034 \$ Back Filter (1 mm)
35 px -0.2034 \$ Additional Filter layer for Al (Front)
36 px 0.2034 \$ Additional Filter layer for Al (Back)
37 px -0.3034 \$ Badge Identification plate
38 px 0.3034 \$ Back of Badge

C

C *** Savannah Dosimeter z axis planes

44 pz -2 \$ Lower Boundary of Filter Set
45 pz -1 \$ Mid boundary of filter set
46 pz 0 \$ Separation between filter set and Pb Identification
49 pz 2 \$ Upper boundary of Pb identification
51 pz -2.25 \$ Lower boundary of dosimeter
52 pz 4.75 \$ Upper boundary of dosimeter

C

C PMMA Phantom

61 rpp 0.4034 15.4034 -15 15 -15 15 \$ PMMA Phantom

C

89 so 30 \$ Outer Air Sphere

C Data Cards

C

C ***** Material Cards

C *** Dry Air: Density = 1.205e-3 g/cc (ICRU 37, 1984)

m204 7000 -0.755636 \$air (US S. Atm at sea level)
8000 -0.231475
18000 -0.012889

C

C *** Aluminum (Al) p=2.6989 g/cm3

m208 13000 -1 \$aluminum

ATTACHMENT C
FILM BADGE MODEL
Page 3 of 6

C
C *** Lead (Pb) 11.35 g/cm3
m252 82000 -1 \$lead
C
C *** Silver (Ag) p=10.50 (Natural)
m7 47000 -1 \$silver
C
C *** PMMA *** (Lucite)
m8 1000 -0.080538 \$PMMA
6000 -0.599848
8000 -0.319614
C
C *** Alumized Mylar p=1.39g/cm3
m9 1000 -0.03679458 \$aluminized mylar
6000 -0.5480593
8000 -0.2920269
13000 -0.1231192
C
C *** Cellulose p=1.42 g/cc
m3 1000 -0.062162 \$cellulose
6000 -0.444462
8000 -0.493376
C
C *** DuPont Type 555 film emulsion, density = 1.4
m2 1000 -0.0952 \$H
6000 -0.707 \$C
7000 -0.238 \$N
8000 -0.3528 \$O
35000 -0.3926 \$Br
47000 -0.53 \$Ag
C
C *** Nylon (Plastic) 1.14 g/cm3
m4 1000 -0.097976 \$Nylon (plastic)
6000 -0.636856
7000 -0.123779
8000 -0.141389
mode p e
C
C Importances, using a multiplier of 2 between layers approaching film
C
imp:p
32 \$ Cell 21, Film (Pb region)
32 \$ Cell 22, Film (Ag region)
32 \$ Cell 23, Film (Air region)
32 \$ Cell 24, Film (Al region)
32 \$ Cell 25, Film (Nylon region)
16 \$ Cell 28, Front Mylar
16 \$ Cell 29, Back Mylar
8 \$ Cell 31, Front Filter (Pb)

ATTACHMENT C
FILM BADGE MODEL
 Page 4 of 6

```

8      $ Cell 32, Front Filter (Ag)
8      $ Cell 33, Front Open Filter (Air)
8      $ Cell 34, Front Filter (Al)
8      $ Cell 35, Front Filter (Nylon)
4      $ Cell 36, Air Volume Above Additional Al thickness
4      $ Cell 37, Air Volume Beside additional Al thickness
4      $ Cell 38, Additional 1 mm Al thickness
2      $ Cell 39, Plastic Identification Cover
8      $ Cell 41, Front Filter (Pb)
8      $ Cell 42, Front Filter (Ag)
8      $ Cell 43, Front Open Filter (Air)
8      $ Cell 44, Front Filter (Al)
8      $ Cell 45, Front Filter (Nylon)
4      $ Cell 46, Air Volume Above Additional Al thickness
4      $ Cell 47, Air Volume Beside additional Al thickness
4      $ Cell 48, Additional 1 mm Al thickness
2      $ Cell 49, Plastic Identification Cover
1      $ Cell 52, Dosimeter Bottom
1      $ Cell 53, Dosimeter Top
1      $ Cell 54, Dosimeter Right Side
1      $ Cell 55, Dosimeter Left Side
1      $ Cell 61, PMMA Phantom
1      $ Cell 98, Air Volume
0      $ Cell 99, Outside Universe

```

C

C Source, as flat plane directly in front of badge

C

```

sdef   pos -0.5 0 0
        rad=d4           $ Starting position, radius for disk
        axs -1 0 0
        ext=0.0          $ disk source is a cylinder source w/ 0.0 extent
        vec 1 0 0
        dir=1.0
        erg=D10          $ Use spectra from Geometry runs
si4 H 0.0 4
sp4 -21 1
#      si10    sp10
        H             D
        0             0
        0.010       2.40699E-17
        0.020       1.83079E-16
        0.030       1.06860E-14
        0.040       5.38261E-14
        0.050       8.88216E-14
        0.060       1.04498E-13
        0.070       1.05721E-13
        0.080       9.86906E-14
        0.090       8.55548E-14
        0.100       7.87470E-14

```

ATTACHMENT C
FILM BADGE MODEL
Page 5 of 6

0.110	6.40245E-14
0.120	5.59481E-14
0.130	4.85688E-14
0.140	3.98014E-14
0.150	3.58915E-14
0.160	3.22578E-14
0.170	2.97443E-14
0.180	2.59220E-14
0.190	2.36927E-14
0.200	1.96994E-14
0.210	1.84759E-14
0.220	1.73283E-14
0.230	1.69887E-14
0.240	1.55532E-14
0.250	1.53104E-14
0.300	6.66064E-14
0.350	5.06615E-14
0.400	4.93796E-14
0.450	3.62498E-14
0.500	3.44993E-14
0.600	6.11587E-14
0.700	2.51803E-14
0.800	1.49166E-14
0.900	2.07992E-15
1.000	3.54375E-15
1.100	1.98845E-15
1.200	1.52424E-15
1.300	9.79980E-16
1.400	9.43520E-16
1.500	7.79964E-16
1.600	5.92042E-16
1.700	2.58030E-16
1.800	2.37523E-16
1.900	1.39327E-16
2.000	1.04503E-16
2.100	1.80974E-16
2.200	2.29078E-15

C

C Tallys

C

f6:e 21**fm6 1.602E-10 \$ convert (MeV per g) to J per kg****fc6 Pb Region, J/kg per source photon**

C

f16:e 22**fm16 1.602E-10 \$ convert (MeV per g) to J per kg****fc16 Ag Region, J/kg per source photon**

C

f26:p 23

ATTACHMENT C
FILM BADGE MODEL
Page 6 of 6

```
fm26 1.602E-10 $ convert (MeV per g) to J per kg
fc26 Air Region, J/kg per source photon
C
f36:e 24
fm36 1.602E-10 $ convert (MeV per g) to J per kg
fc36 Al Region, J/kg per source photon
C
f46:e 25
fm46 1.602E-10 $ convert (MeV per g) to J per kg
fc46 Nylon Region, J/kg per source photon
C
C
nps 1E8
```